

Distinct medial amygdala oxytocin receptor neurons projections respectively control consolation or aggression in male mandarin voles



Open Access This file is licensed under a Creative Commons Attribution 4.0 International License, which permits use, sharing, adaptation, distribution and reproduction in any medium or format, as long as you give appropriate credit to the original author(s) and the source, provide a link to the Creative Commons

license, and indicate if changes were made. In the cases where the authors are anonymous, such as is the case for the reports of anonymous peer reviewers, author attribution should be to 'Anonymous Referee' followed by a clear attribution to the source work. The images or other third party material in this file are included in the article's Creative Commons license, unless indicated otherwise in a credit line to the material. If material is not included in the article's Creative Commons license and your intended use is not permitted by statutory regulation or exceeds the permitted use, you will need to obtain permission directly from the copyright holder. To view a copy of this license, visit

<http://creativecommons.org/licenses/by/4.0/>.

REVIEWER COMMENTS

Reviewer #1 (Remarks to the Author):

The study presents a series of stepwise, perhaps even eloquent, experiments showing regional connections, manipulation of neurons, expression and then activation of using optogenetics and pharmaceutical silencing to refine and understand the role of the medial amygdala and specifically neurons that express oxytocin receptors in the anterior insula and ventral lateral ventral medial hypothalamus. The findings indicate that subgroups of oxytocin receptor expressing neurons within the MeA may be involved in the regulation of both aggression and prosocial interactions dependent upon the group and the region they innervate. While very interesting and potentially significant finding, the article is dense and there are significant grammatical issues that make it very challenging to fully interpret the findings. These need to be corrected throughout the manuscript.

While this does not require detailed methods, which appear in the methods section following the Discussion, the introduction needs to include discussion of the series of experiments run and the purpose/flow. A flow chart would be extremely helpful. This is essential because of the very detailed experiments. Behavioral measure should also be indicated, although this may be a separate table or chart.

Grammar issues throughout the manuscript. There are way too many to try and point them all out. The first three lines of the abstract indicate the issues.

"The individuals often show consolation to distressed companion or show aggression to the intruder displaying behavioral flexibility" (The way this is worded indicates that they show behavioral flexibility to intruders. Animals are well known for display differential behaviors depending upon circumstances and the individual that the behaviors are directed towards).

The circuit mechanisms underlying switch (switching) between consolation and aggression remain unclear.

In the present study, using high socially mandarin voles (can be highly social, but not socially mandarin voles).

First line of the introduction

"anti-social behaviors respectively in animals and human." Humans are animals and human should be plural.

2nd line of introduction

"they encountering displaying behavioral flexibility" This is not grammatically correct.

3rd line

The flexibility that individuals display optimal behavioral responses in different social context are both (remove both as both means two and there are three well-being, survival and stability) crucial for individual well-being, survival and stability of mammal species^{1, 2}.

2nd paragraph Oxytocin should not be capitalized.

Line 69 introduction

"Socially male". Here as a modifier socially suggests that maleness is defined by social interactions not genetics or anatomy. Therefore the test subjects could be females who if they displayed the correct behaviors would be socially male.

In addition to grammar unusual terminology is frequently used. Two examples below.

Discussion multidisciplinary approach. While they use a number of different techniques they are not multidisciplinary.

From the methods.

The consolation test procedure “as same as previously” described 7, was used to evaluate “one’s” prosocial level. Briefly, male subject cohobited with a “contemporary” same-sex sibling after weaning – if they are the same sex siblings, they must by definition be the same age. What does contemporary mean in this context?

Reviewer #2 (Remarks to the Author):

In this study, the authors examined the role of MeA OXTR cells that project to the anterior insula and VMHvl in allogrooming and aggression. Through ablation, chemogenetic inhibition, optogenetic activation and fiber photometry recording, they showed that MeA OXTR-AI cells modulate allogrooming, whereas MeA OXTR-VMHvl cells modulate male aggression. The authors further showed that MeA OXTR-VMHvl and MeA OXTR-AI cells are primarily glutamatergic. The functional and recording results are largely convincing, but there is an important conceptual discrepancy that makes the results perplexing. MeA –VMHvl and MeA –AI cells appear to overlap extensively. 70% of MeA –VMHvl cells also project to AI, but yet they appear to mediate distinct behaviors and show very different response patterns. How could this happen? Furthermore, some essential tools used in the study are not fully characterized, e.g. OXTR antibody, OXTR promoter driven virus, Vglut2 antibody. These tools are prone to problems and need to be thoroughly characterized before using for addressing new biological questions.

Here are some specific comments:

1. Figure S2: please quantify the c-Fos level after aggression in AI and after consolation in the VMHvl. Comparison between consolation and aggression groups help understand whether the c-Fos pattern is specific to a social context or simply reflect exposure to a social target.
2. Figure S2: For MeA, please analyze MeApd and MeApv separately. After consolation and aggression, the c-Fos expression pattern looks different in these two subregions.
3. Figure 1: AAV1 travels both retrogradely and anterogradely. For figure 1e-n, it is not clear whether the GFP cells are retrogradely or anterogradely labeled. Again, please show the Fos+EGFP+ cells in VMHvl and AI after both consolation and aggression.
4. Figure S3: Given that this is not a widely used commercial antibody, its utility should be verified, ideally using KO animals. The OXTR staining in the OXTR appears to be very dense, making one wonder whether the staining is specific to OXTR cells. The antibody generated in Froemke lab was used for mice, it was not validated in voles.
5. Figure 2a-e: if the antibody works well, it is not clear why the OXTR is labeled using AAV-OXTR-mCherry. Based on Figure S3, the virus seems to only label a small fraction of OXTR cells. Thus, this strategy does not capture OXTR expression accurately. Why not just use the OXTR antibody?
6. Figure 2f-s: please confirm the cell death by examining OXTR staining in the MeA after Cap3 vs. GFP injection. The lack of EGFP expression in MeA could be due to cell death or failed virus expression.
7. Figure 2f-2s, the clean behavior separation after killing MeA OXTR cells projecting to VMHvl vs. AI is surprising. Given that there is a substantial overlap between MeA cells projecting to VMHvl and AI. According to Figure 1c and 1d, 10% of MeA cells projecting to VMHvl and 7% projecting to both VMHvl and AI, meaning that MeA-AI cells include 70% of MeA-VMHvl cells. Thus, it is surprising that when MeA-AI cells are killed, which should also kill 70% of MeA-VMHvl cells, aggression does not change.
8. Figure 3d, e, n, o: the representative traces are of very different scales. Are the GCaMP6 signals of MeA OXTR-AI cells much weaker than that of MeA OXTR-VMHvl cells? If so, please explain especially given that there are more MeA cells projecting to AI than to the VMHvl.
9. Figure 3b and i: please indicate the optic fiber placement. Are the recordings from dorsal or ventral MeA? This is important considering that they are very different behavior functions.
10. Figure 3a-j: the lack of increase of MeA OXTR-Ai cells is again somewhat surprising given that AI projecting cells largely cover VMHvl projecting cells. Please discuss.
11. Figure 3: AUC analysis is not fair to all behaviors. For example, sniffing object episode is likely to be a lot shorter than 4s, thus 0-4s window will include periods that the behavior do not occur. The duration of the behavior episode should be taken into the consideration when analyzing the fiber photometry data.
12. Figure S7: again, it is not clear why AAV-OXTR-mCherry is used instead of antibody. The antibody staining will be more straightforward and comprehensive. The number of virus infected cells is low. All figures should be better labeled to indicate what each color represents.
13. Figure 5: It is surprising that MeA OXTR cells that project to VMHvl and AI are primarily

glutamatergic as MeA, especially its dorsal region, contains mainly GABAergic cells. MeA GABAergic cells but not glutamatergic cells promote inter-male aggression. The signal of antibody staining in Figure 5a is hardly convincing. In the text, it claims that Figure 5a and 5c show both Vglut2 and GABA staining, but only Vglut2 staining should be found in the figure. Please quantify the GABAergic vs. glutamatergic cells in the vole MeA as there might be species difference. Antibody often does not work as it should. It is important to validate the antibody. The authors may also consider using in situ hybridization to validate the neurotransmitter type of the cells.

14. Figure 5h-k, is there any monosynaptic IPSC evoked by the light?

15. Given that MeA OXTR-AI and MeA Tac1/GABA-MPOA activation generates very similar behavior phenotype, the authors need to address whether these two are largely overlapping or distinct. Please consider perform dual retrograde labeling from AI and MPOA and examine the extent of overlap at MeA. Or examine the overlap between Tac1/GABA and MeA OXTR-AI cells.

16. The reviewer suggest the authors to remove the detailed stats in the main text as it makes the paper hard to read.

Reviewer #3 (Remarks to the Author):

This study focuses on understanding the circuit mechanisms that control the switch between consolation and aggression in highly social mandarin voles. The authors identified two distinct subtypes of oxytocin receptor (OXTR) neurons in the medial amygdala (MeA) that project to the anterior insula (AI) and ventromedial hypothalamus (VMHvl). These neurons respond differently to stressed siblings or unfamiliar intruders. By manipulating these pathways, the researchers observed altered responses to social stimuli. The main type of glutamate receptors involved in these pathways is AMPA receptors in the AI and VMHvl. These findings suggest that the two subtypes of OXTR neurons in the MeA play a crucial role in controlling consolation and aggression. Although this work is potentially interesting, its conceptual advance is limited, and the major conclusions are not convincingly supported by the data. There are a number of major issues concerning the main findings:

1. There is no causal evidence showing if Oxtr neurons are specifically involved in consolation and aggression or if they simply reflect a random subset of neurons that can promote these behaviors. Indeed, previous studies have shown that tachykinin neurons in the MeA mediate consolation and tachykinin-negative neurons mediate aggression (Wu et al 2021). This suggests that Oxtr neurons are likely not a specific population for these behaviors.

2. The authors need to validate the viral tools used for retrograde labeling in mandarin voles and to make sure that AAV(retro) indeed labels neurons in a retrograde manner. Although these tools are known to work well in mice, they may not work in the same manner in mandarin voles. Previous studies show that viral vectors work very differently across species. The authors also need to rule out the possibility that this AAV(retro) may label neurons in an anterograde manner (anterograde transsynaptic labeling). The cells labeled in Figure 1i and 1j look very broad and non-specific.

3. Since Vglut2 is only expressed in a subset of Oxtr neurons (Fig. 5b), it is unclear if Oxtr neurons mediate consolation and aggression through a glutamatergic mechanism. The authors should confirm this by directly manipulating glutamatergic neurons in the MeA or glutamatergic Oxtr neurons in the MeA.

4. The authors performed optogenetic activation of MeA neuron terminals in the VMHvl and AI. However, they didn't show any behavioral phenotypes that are associated with these manipulations. To support the main conclusion of this study, it is essential to determine if optogenetic activation of MeA neuron terminals in the VMHvl and AI produces a similar behavioral phenotype.

5. The retrograde labeling from VMHvl and AI in the MeA labels neurons that may also project collaterally to other brain areas. The fact that activating retrogradely labeled cell bodies can promote a behavior does not necessarily mean that it is the MeA-VMHvl or MeA-AI projections that mediate these behavioral functions. The authors should perform experiments to rule out the involvement of other collateral projections of these two neuronal populations in consolation and aggression.

6. The authors should express a fluorescent marker in MeA Oxtr neurons, confirm if they can identify axonal terminals in VMHvl, AI and other brain regions such as the BNST and the preoptic area, and quantify the axon projection density of these neurons in these brain areas.

7. The percentage of Oxtr neurons shown in Fig. 2e seems to be substantially higher than what was shown in the representative images in Fig. 2b, particularly outside the boxes. This questions the validity of the quantification. The authors should also show more representative images from different areas of the MeA in higher magnification.

8. In light of the recent paper indicating that Oxtr is not required for social attachment in voles (Berendzen et al 2023), it is important to perform additional experiments to examine and confirm the functional involvement of Oxtr and the oxytocin signaling in these Oxtr-expressing neurons during consolation and aggression.

Author Rebuttals to Initial Comments:

Response to all reviewers:

We thank all reviewers for their valuable comments on our manuscript. Based on the reviewers' comments and suggestions, we have performed the following additional experiments in the last several months that delayed the resubmission:

- (1) RNAscope Multiplex Fluorescent v2 Assay combined with Immunofluorescence (Integrated Co-detection Workflow (ICW)) was used to validate the efficiency and specificity of OXTR antibody. The detailed results were presented in the revised manuscript and responses to the comments.
- (2) Fluorescent anterograde monosynaptic tracer (rAAV-CAG-mWGA-mCherry) combined with c-Fos labeling was used to map activities of post-synaptic (the AI and VMHvl) neuron projected from the MeA during different behaviors.
- (3) AAVs (2/R) instead of CTBs, and OXTR antibody instead of rAAV-OXTR-mCherry were used to explore the morphological distribution of the populations of MeA OXTR neurons that project to AI or VMHvl respectively.
- (4) Densities of fibers of MeA OXTR neurons in the AI, MPOA, VMHvl and BNST were quantified.
- (5) Anti-OXTR staining in the MeA was used to confirm the cell death caused by expression of AI / VMHvl-retro Caspase-3 virus in the MeA.
- (6) Real-time OXT release in the MeA and PVN^{OXTR+MeA} activity upon consoling and attacking were measured using OXT sensor1.0 and GCaMp virus respectively, and were detected by fiber photometry.
- (7) Levels of consolation and aggressive behaviors were measured while fibers of the (glutamatergic) MeA^{OXTR+AI} and MeA^{OXTR+VMHvl} neurons were activated using optogenetic method.

Additionally, we also:

- (1) re-analyzed data of AUC per second from fiber photometry recording;
- (2) revised the grammatical issues as reviewer suggested;
- (3) added the brief description of series of experiments run and the purpose in the introduction as suggested;
- (4) moved the detailed stats in the main text to the supplementary files.

Finally, we performed several additional experiments to specifically address reviewers' questions. For example, we

- (1) quantified the c-Fos positive neurons in the AI after aggression and in the VMHvl after consolation;
- (2) analyzed the numbers of c-Fos positive neurons in the MeApd and MeApv separately;
- (3) quantified the percentages of c-Fos⁺EGFP(AAV1 tracer)⁺ neurons in the AI after aggression and that in the VMHvl after consolation;
- (4) added an experimental flow chart and a table of behavioral measure.

We believe these new data and analyses have significantly strengthened and expanded our original conclusions, and consequently improve our work. We would like to thank the reviewers again for taking the time to review our manuscript.

Point-to-point responses:

(Reviewers' comments in Blue; Our responses in Black)

PS: All changes in the revised manuscript text file are marked with red underline.

Reviewer #1 (Remarks to the Author):

The study presents a series of stepwise, perhaps even eloquent, experiments showing regional connections, manipulation of neurons, expression and then activation of using optogenetics and pharmaceutical silencing to refine and understand the role of the medial amygdala and specifically neurons that express oxytocin receptors in the anterior insula and ventral lateral ventral medial hypothalamus. The findings indicate that subgroups or oxytocin receptor expressing neurons within the MeA may be involved in the regulation of both aggression and prosocial interactions dependent upon the group and the region they innervate. While are very interesting and potentially significant finding, the article is dense and there are significant grammatical issues that make it very challenging to fully interpret the findings. These need to be corrected through out the manuscript.

Response: Thanks for your suggestion.

To make our article concise, clear and readable, we took the following strategies:

- 1) Detailed stats and source data in the main text have been moved to the supplementary files.
- 2) Some main figures have been reorganized and some figures that are not very important and not closely associated with main topic have been removed from supplementary figures.
- 3) We have carefully checked the manuscript throughout and some grammatical errors have been found and corrected. We believe the language of the manuscript have been improved.

While this does not require detailed methods, which appear in the methods section following the Discussion, the introduction needs to include discussion of the series of experiments run and the purpose/flow. A flow chart would be extremely helpful. This is essential because of the very detailed experiments. Behavioral measure should also be indicated, although this may be a separate table or chart.

Response: Thanks for your suggestion. Following revisions have been made.

- 1) The series of experiments run and the purpose were described in the last paragraph of introduction in the revised manuscript (**Pages 3, line 72-90**). Corresponding summary figure was also added (**Fig. S1 in manuscript**) as follows.
- 2) In every main figure, a flow chart with experimental procedure had been added in the revised manuscript (In revised manuscript, **Fig. 1b** for co-labeling of the MeA^{AI} and MeA^{VMHvl}; **Fig. 1f** for AAV(2/1) strategy; **Fig. S5a** for CAG-mWGA strategy; **Fig. 2b** for co-labeling of the MeA^{OXTR+AI} and MeA^{OXTR+VMHvl}; **Fig. 2f** for ablation of the MeA^{OXTR+AI} and MeA^{OXTR+VMHvl}; **Fig.S11a** for MeA^{OXT} sensor, **Fig S11h** for GCaMP-PVN^{OXT+MeA}, **Fig. 3a / k** for GCaMP-MeA^{OXTR+AI} / GCamp-MeA^{OXTR+VMHvl}; **Fig. 4b and Fig. 6m** for optogenetic activation of the (glutamatergic) MeA^{OXTR+AI} and MeA^{OXTR+VMHvl} somata (fibers); **Fig. 5a** for pharmacogenetic inhibition of the MeA^{OXTR+AI} and MeA^{OXTR+VMHvl}).
- 3) Behavioral measure has been indicated as a table in revised manuscript (**Table. S1 in**

manuscript) as follows.

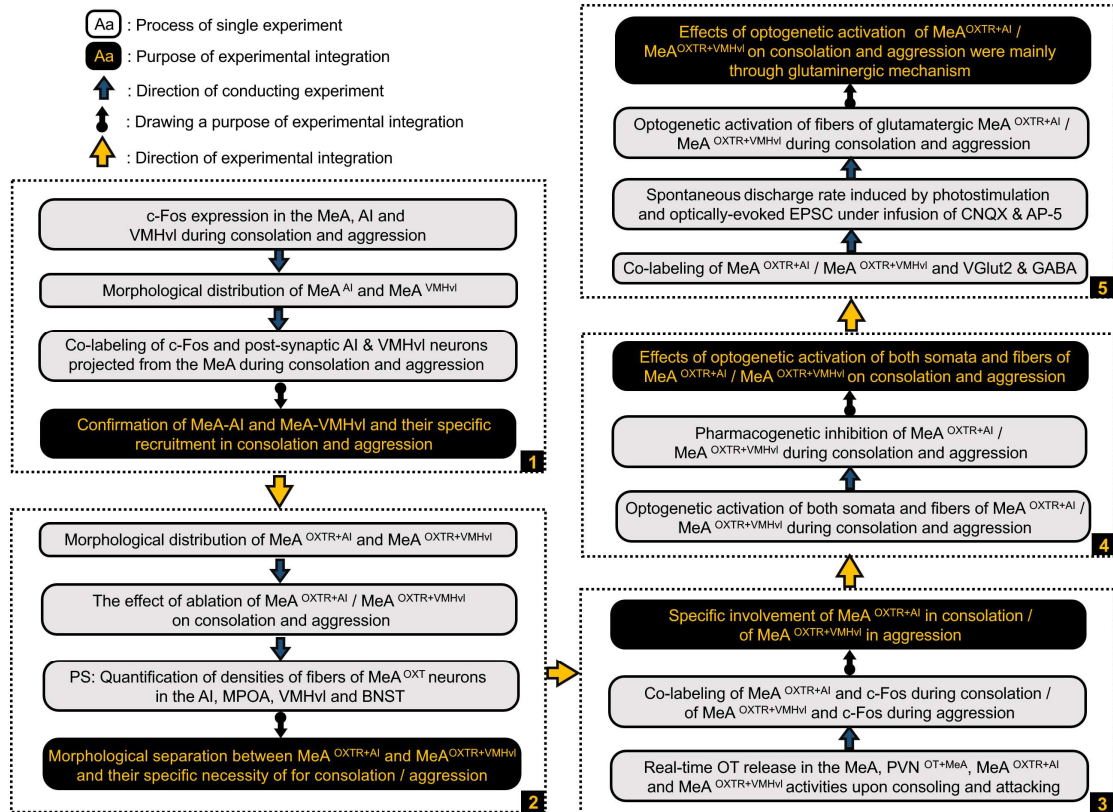


Fig. S1 The flow chart of experimental run and corresponding purpose in the present study.

Behavioral test	indicators	Definition for recording / measuring
Consolation test	Sniff sibling	Using nose to inspect any portion of the sibling's body, including the nose, head, tail and anogenital areas.
	Allogroom sibling	Head contact with the body or head of subjects' sibling, accompanied by a rhythmic head movement.
Resident-intruder paradigm	Sniffing intruder	Using nose to inspect any portion of the intruder's body, including the nose, head, tail and anogenital areas.
	Attack intruder	A series of actions initiated by the subjects to the intruders, including body swaying back and forth for claiming lordship, bites, pinning, tumbling and quick chasing for attack or eviction between these behaviors.
New object recognition model	Sniff object	Using nose to inspect the surface of object (rubik's cube).

Table. S1 Definition of main behavioral indicators in consolation test, resident-intruder paradigm and new object recognition model.

Grammar issues throughout the manuscript. There are way too many to try and point them all out. The first three lines of the abstract indicate the issues:

“The individuals often show consolation to distressed companion or show aggression to the intruder displaying behavioral flexibility” (The way this is worded indicates that they show behavioral flexibility to intruders. Animals are well known for display differential

behaviors depending upon circumstances and the individual that the behaviors are directed towards).

Response: Thanks for your careful checking. This error has been corrected in the revised manuscript (**Pages 1, line 5-6**).

The circuit mechanisms underlying switch (switching) between consolation and aggression remain unclear.

Response: Thanks for your careful checking. This error has been corrected in the revised manuscript (**Pages 1, line 6-7**).

In the present study, using high socially mandarin voles (can be highly social, but not socially mandarin voles).

Response: Thanks for your careful checking. This error has been corrected in the revised manuscript (**Pages 1, line 7**).

First line of the introduction

“anti-social behaviors respectively in animals and human.” Humans are animals and human should be plural.

Response: Sorry for this problem. This error has been corrected in the revised manuscript (**Pages 2, line 27**).

2nd line of introduction

“they encountering displaying behavioral flexibility” This is not grammatically correct.

Response: Thanks for your careful checking. This error has been corrected in the revised manuscript (**Pages 2, line 28**). “Encountering” has been changed into “encounter”.

3rd line

The flexibility that individuals display optimal behavioral responses in different social context are both (remove both as both means two and there are three well-being, survival and stability) crucial for individual well-being, survival and stability of mammal species^{1, 2}.

Response: Thanks for your careful checking. This error has been corrected in the revised manuscript (**Pages 2, line 29**). The word “both” has been removed.

2nd paragraph Oxytocin should not be capitalized.

Response: Thanks. This error has been corrected in the revised manuscript (**Pages 2, line 35**).

Line 69 introduction

“Socially male”. Here as a modifier socially suggests that maleness is defined by social interactions not genetics or anatomy. Therefore the test subjects could be females who if they displayed the correct behaviors would be socially male.

Response: Sorry for the confusing. Here, I just want to describe that mandarin voles are highly social species. This sentence has been reorganized as “In mandarin voles (*Microtus mandarinus*), males often display high levels of consolation to partners, but intensive

aggression to unfamiliar intruders. Thus, males of this species were used in the present study" (**Pages 3, line 70-72**).

In addition to grammar unusual terminology is frequently used. Two examples below. Discussion multidisciplinary approach. While they use a number of different techniques they are not multidisciplinary.

Response: Thanks for your careful checking. As reviewer suggested, "multidisciplinary approach" was replaced by "a number of different techniques" (**Pages 25, line 517**).

From the methods.

The consolation test procedure "as same as previously" described 7, was used to evaluate "one's" prosocial level. Briefly, male subject cohabited with a "contemporary" same-sex sibling after weaning – if they are the same sex siblings, they must by definition be the same age. What does contemporary mean in this context?

Response: Sorry for the confusing. "one's" has been changed into "subject voles" (**Pages 37, line 972**); The word "contemporary" has been removed (**Pages 37, line 973**).

Point-to-point responses:

(Reviewers' comments in Blue; Our responses in Black)

PS: All changes in the revised manuscript text file are marked with red underline.

Reviewer #2 (Remarks to the Author):

In this study, the authors examined the role of MeA OXTR cells that project to the anterior insula and VMHvl in allogrooming and aggression. Through ablation, chemogenetic inhibition, optogenetic activation and fiber photometry recording, they showed that MeA OXTR-AI cells modulate allogrooming, whereas MeA OXTR-VMHvl cells modulate male aggression. The authors further showed that MeA OXTR-VMHvl and MeA OXTR-AI cells are primarily glutamatergic. The functional and recording results are largely convincing, but there is an important conceptual discrepancy that makes the results perplexing. MeA –VMHvl and MeA –AI cells appear to overlap extensively. 70% of MeA –VMHvl cells also project to AI, but yet they appear to mediate distinct behaviors and show very different response patterns. How could this happen? Furthermore, some essential tools used in the study are not fully characterized, e.g. OXTR antibody, OXTR promoter driven virus, Vglut2 antibody. These tools are prone to problems and need to be thoroughly characterized before using for addressing new biological questions.

Response: Thanks for your positive comments. In the original version of the manuscript, some inconsistent results really made reader confusing and perplexing. To address these issues and make the result more convincing, many additional experiments were conducted and relevant results were added. The detailed responses are presented as following:

1) In the original manuscript, using CTB for retrograde tracing, it is found that MeA OTR neurons that project to AI or VMHvl were largely overlapped, but control consolation and aggression specifically. This result is really confusing. Through discussion with and consulting experts from company that supplies virus tool, it is found that although CTB can retrogradely trace brain areas in a short time, large dose of CTB injection with long time can result in diffusion of CTB from upstream target neurons to adjacent local neurons that may cause no-specific CTB marking of neurons. It is difficult to determine optimum dose and time for CTB injection. That may be the reason that MeA OTR neurons that project to AI or VMHvl were largely overlapped using CTB for retrograde tracing.

To resolve this problem, retrograde tracing virus (AAVs (2/R)) with different fluorescence instead of CTB and OXTR antibody instead of rAAV-OXTR-mCherry were used to mark MeA OXT neurons that project to AI or VMHvl respectively. In revised manuscript, the result showed that MeA neurons projecting to AI (MeA^{AI}) and MeA neurons projecting to VMHvl (MeA^{VMHvl}) (**Fig. 1a ~ e in manuscript**), or MeA OTR neurons projecting to AI (MeA^{OXTR+AI}) and MeA OTR neurons projecting to VMHvl (MeA^{OXTR+VMHvl}) neuronal populations (**Fig 2a ~ e in manuscript**) are morphologically separated, which is common in different bregma sites as well as in different subregions in the MeA. Although the infection and expression of AAVs (2/R) viruses spent long time, they do not diffuse as CTB dyes, so the results obtained with the new virus strategy are convincing.

2) The OXTR antibody was synthesized entirely in accordance with that used by Professor

Robert Froemke based on homologous OXTR amino acid sequence of voles according to epitope sequences from mice: KLH-CYS-EGSAAGGAGRAALARVS SVKLISKAKI (**see method, pages 39, line 1065-1069**). Therefore, the present antibody is fully applicable and specific to the OXTR of Mandarin voles. Then RNAscope Multiplex Fluorescent v2 Assay combined with Immunofluorescence (Integrated Co-detection Workflow (ICW)) was used to validate the efficiency and specificity of OXTR antibody. The result showed that ~ 97% of OXTR mRNA positive neurons were marked by OXTR antibody and ~ 97% of OXTR antibody positive neurons were labeled by OXTR mRNA displaying high efficiency and specificity of OXTR antibody (**Fig. S6 in manuscript, the gene sequence of OXTR in mandarin voles is attached to the end of this letter**). Thus, it is suggested that the results that used OXTR antibody to label OTR neurons or validate OXTR promoter driven virus are convincing.

3) To verify the results of the VGlut2 antibody staining, the MeA^{OXTR+AI} and MeA^{OXTR+VMHvl} neurons were infected with rAAV-DIO-hM4D(Gi)-mCherry and labeled with GABA antibody (**Fig. 6a ~ d in manuscript**). It is found that ~ 20% and ~ 24% of the MeA^{OXTR+AI} and MeA^{OXTR+VMHvl} neurons was GABA positive. It is consistent with result the VGlut2 antibody staining that the main types of MeA^{OXTR+AI} and MeA^{OXTR+VMHvl} are glutamatergic neuron.

Here are some specific comments:

1. [Figure S2](#): please quantify the c-Fos level after aggression in AI and after consolation in the VMHvl. Comparison between consolation and aggression groups help understand whether the c-Fos pattern is specific to a social context or simply reflect exposure to a social target.

Response: We appreciate your valuable suggestion very much. As showed in **Fig. S3e ~h and S3i ~ l in manuscript**, the c-Fos positive neurons in the AI after aggression and the c-Fos positive neurons in the VMHvl after consolation were counted respectively and added in **pages 4, line 117 and 119**. It is found that aggression did not induce significant increase of c-Fos level in the AI and consolation did not enhance the c-Fos level in the VMHvl indicating specific patterns of neuron activities to a different social context.

2. Figure S2: For MeA, please analyze MeApd and MeApv separately. After consolation and aggression, the c-Fos expression pattern looks different in these two subregions.

Response: Thanks for your suggestion. As showed in Fig. S3a ~ d in manuscript, we have analyzed MeApd and MeApv subregions separately. Both PV and PD showed increased c-Fos expression upon consoling and attacking. Corresponding results text was showed in pages 4, line 112-115.

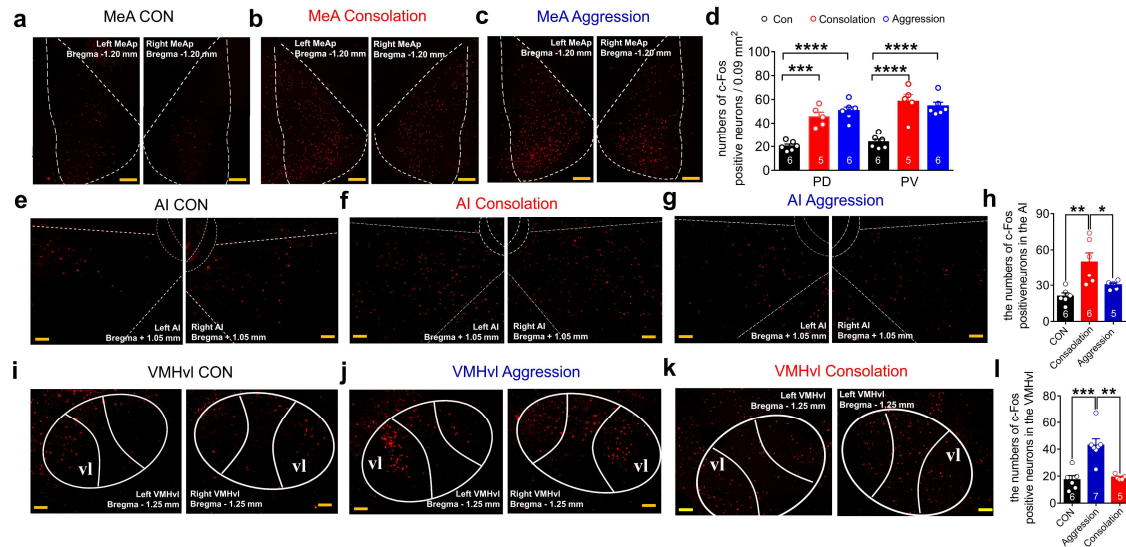


Fig. S3 in manuscript. Effect of consolation and aggression on c-Fos expression in the AI, VMHvl and MeA neurons. (a ~ c) Representative images of c-Fos (red) positive cells in the bilateral MeA after the control treatment (CON, $n = 6$ voles) (a), consolation test (Consolation, $n = 5$ voles) (b) and resident-intruder paradigm (Aggression, $n = 6$ voles) (c). scale bars, 200 μ m. (d) The quantitative distinction of numbers of c-Fos positive cells in the posterior dorsal (PD) and posterior ventral (PV) subregions between the CON, Consolation and Aggression groups. (e ~ g) Representative images of c-Fos positive cells in the bilateral AI in the CON ($n = 6$ voles) (e), Consolation ($n = 6$ voles) (f) and Aggression ($n = 5$ voles) (g) groups. scale bars, 100 μ m. (h) The quantitative distinction of the numbers of c-Fos positive cells in the AI between the CON, Consolation and Aggression groups. (i ~ k) Representative images of c-Fos positive cells in the bilateral VMHvl in the CON ($n = 6$ voles) (i), Aggression ($n = 7$ voles) (j) and Consolation ($n = 5$ voles) (k) groups. scale bars, 100 μ m. (l) The quantitative distinction of the numbers of c-Fos positive cells in the VMHvl among the Con, Consolation and Aggression groups. **** $p < 0.0001$, *** $p < 0.001$, ** $p < 0.01$, * $p < 0.05$. All error bars = s.e.m.

3. Figure 1: AAV1 travels both retrogradely and anterogradely. For figure 1e-n, it is not clear whether the GFP cells are retrogradely or anterogradely labeled. Again, please show the Fos+EGFP+ cells in VMHvl and AI after both consolation and aggression.

Response: Thanks for your rigorous consideration.

1) According to previous reports, AAV (2/1) may indeed have property of retrograde labeling¹,², that is, its property of anterogradely across single-synapses labeling is not very strict. However, AAV (2/1) was still used for anterograde labeling in recent study by Dayu Lin that is published in Nature titled Antagonistic circuits mediating infanticide and maternal care in female mice³. In this study, AAV1-hSyn-Cre and AAV2-hSyn-DIO-mcherry were microinjected into MPOA, several downstream regions were co-labeled with c-Fos antibody and mCherry tracer to reveal involvement of MPOA projections in specific behavior. In addition, Guangjian Qi injected AAV (2/1)-TH-CRE in the NAc and AAV (2/9)-DIO-CHR2 / NpHR / mCherry in the VTA to activate or inhibit dopaminergic NAc-VTA pathway to explore changes in anxiety among animals⁴.

2) In our study, rAAV (2/9)-Ef1 α -DIO-EGFP-WPRE-hGH were injected into the AI or VMHvl, and rAAV (2/1)-hSyn-CRE-WPRE-hGH was injected into the MeA respectively. Compared with virus strategy used by Dayu Lin, this virus strategy used in the present study could exclude retrograde tracing of AAV (2/1) to some extent. In the present study, injection of CRE-AAV (2/1) that anterogradely travel across single synapse in upstream brain region and injection of DIO-EGFP in downstream regions can trace projection of neurons specifically because expression of DIO system is dependent on CRE.

3) In order to further exclude confounding of using AAV1 as anterograde tracer on experimental results, rAAV-CAG-mWGA-mCherry that strictly and anterogradely travel across single synapse was injected into the MeA (**Fig. S5 in manuscript**)⁵, the neuron that co-labeling mCherry tracer and c-Fos in the AI and VMHvl were counted after consolation or aggression. Unpaired T-test analysis revealed that the activities of neuron in the AI and VMHvl that receive projections from MeA during Control, consolation and aggression did not show significant difference between two strategies using AAV (2/1) and CAG-mWGA as anterograde monosynaptic tracer (**Fig. S5k and l in manuscript**). Corresponding results text was showed in **pages 5, line 153-160**; Corresponding methods text was showed in **pages 31, line 746-756**.

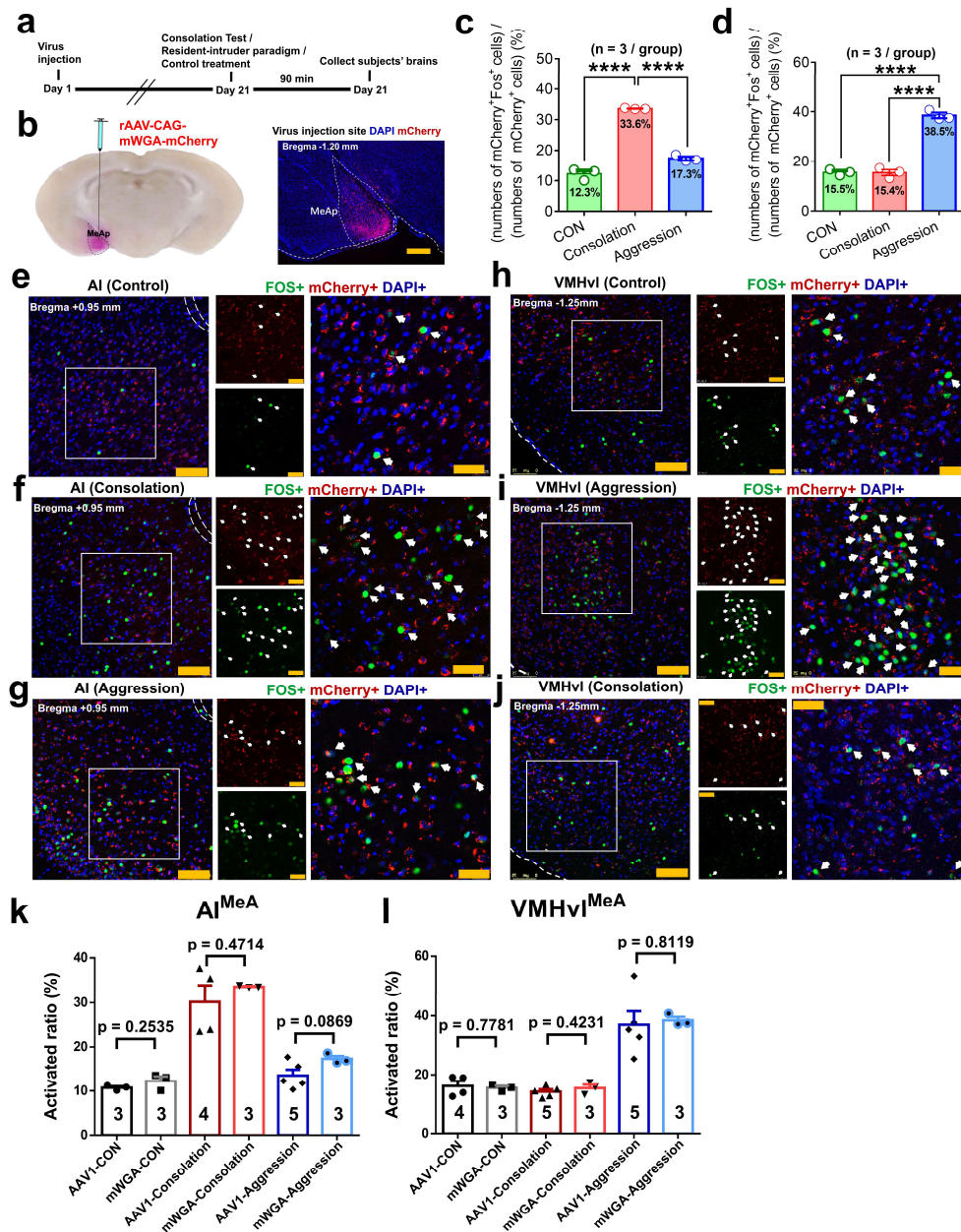


Fig. S5 in manuscript Using fluorescent anterograde trans-synaptic tracer (mWGA-mCherry) and c-Fos labeling to map post-synaptic (the AI and VMHvl) neuronal activity from the MeA during different behaviors. (a and b) Diagram showing injection schedule (up) and site (down) of anterograde monosynaptic labeling virus. (c) Comparison of percentage of mCherry and c-Fos co-labeling AI neurons in whole anterograde virus-marked neurons between the CON, Consolation and Aggression groups. (d) Comparison of percentage of mCherry and c-Fos co-labeling VMHvl neurons in whole anterograde virus-marked neurons between the CON, Consolation and Aggression groups. (e, f and g) Representative overlapped images of anterograde monosynaptic virus (red) and c-Fos (green) at the AI after control treatment (CON, $n = 3$ voles, e), consolation test (Consolation, $n = 3$ voles, f) and resident-intruder paradigm (Aggression, $n = 3$ voles, g). (h, i and j) Representative overlapped images of anterograde virus and c-Fos at the VMHvl after control treatment (CON, $n = 3$ voles, h), consolation test (Consolation, $n = 3$ voles, i) and resident-intruder paradigm (Aggression, $n = 3$ voles, j), respectively. The enlarged views of the selected white boxed areas ($300 \mu\text{m} \times 300 \mu\text{m}$, right), and co-labeling neurons were characterized by white arrows. scale bars, $100 \mu\text{m}$ (left) and $50 \mu\text{m}$ (right). (k) and (l) The distinction of co-labeled c-Fos and fluorescent tracer ratio between AAV (2/1) system and CAG-mWGA strategy in the AI^{MeA} (k) and VMHvl^{MeA} (l). **** $p < 0.0001$. All error bars = s.e.m.

In addition, neurons co-labeling c-Fos and EGFP in the AI after aggression, and that in the VMHvl after consolation were quantified (**Fig. 1 I and m, and p and q in manuscript**), the result showed that more neurons in the AI were activated by consolation and more neurons in the VMHvl were activated by aggression specifically. Corresponding results text was added in **pages 5, line 148 and 151-152**.

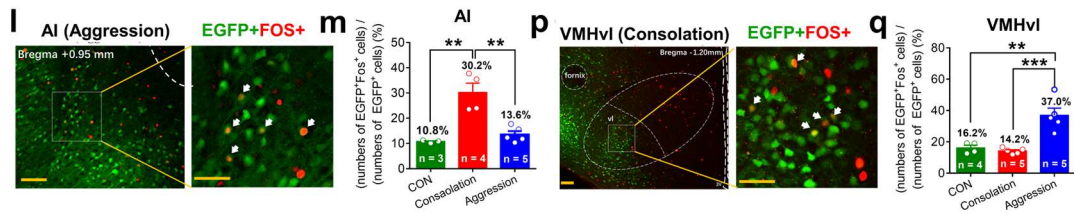


Fig. 1 I and m, and p and q in manuscript The percentage of EGFP and c-Fos co-labeled cells in the AI and the VMHvl under aggression or consolation. *** $p < 0.001$, ** $p < 0.01$. All error bars = s.e.m.

4. Figure S3: Given that this is not a widely used commercial antibody, its utility should be verified, ideally using KO animals. The OXTR staining in the OXTR appears to be very dense, making one wonder whether the staining is specific to OXTR cells. The antibody generated in Froemke lab was used for mice, it was not validated in voles.

Response: Thanks a lot for your professional comment. Noticeably, according to epitope sequences site from mice, we selected homologous OXTR amino acid sequence from voles as epitopes for synthesizing antibody: KLH-CYS-EGSAAGGAGRAALARVS SVKLISKAKI, which is specific and applicable for voles. For verifying the specificity and efficiency of OXTR antibody used in the present study, RNAscope Multiplex Fluorescent v2 Assay combined with Immunofluorescence-Integrated Co-detection Workflow (ICW) was used (**Fig. S6 in manuscript**). The fluorescence probe was constructed according sequence of OXTR gene from mandarin voles. This result showed that the neurons marked by OXTR fluorescence probe were completely overlapped with neuron stained by OXTR antibody. It is suggested that staining with OXTR antibody is specific to OXTR cells. Corresponding results text was indicated in **pages 8, line 194-196**; Corresponding methods text was showed in **pages 31, line 757- pages 32, line 770**.

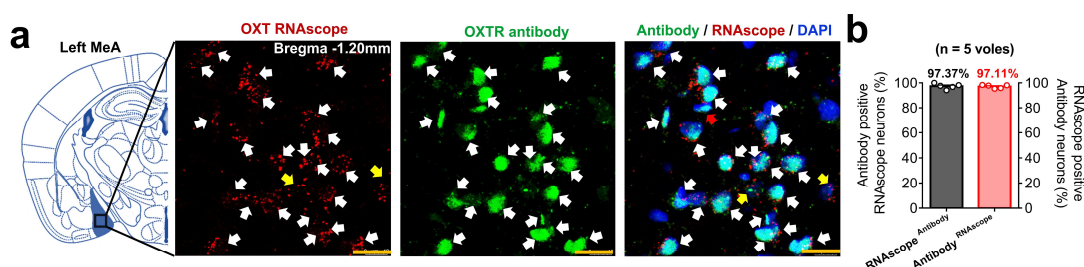


Fig. S6 in manuscript The validation of the efficiency and accuracy of OXTR antibody by RNAscope Multiplex Fluorescent v2 Assay combined with Immunofluorescence-Integrated Co-detection Workflow (ICW). (a) Representative co-labeling images of OXTR RNAscope (AF570, red) and OXTR antibody (AF488, green). Co-labeling neurons were characterized by white arrows. The neurons labeled by antibody but not RNAscope were characterized by red arrows. The neurons labeled by RNAscope but not antibody were characterized by yellow arrows. scale bars, 15 μ m. (b) The percentage of co-labeling neurons in antibody positive neurons and in RNAscope positive neurons, respectively ($n = 5$ voles). All error bars = s.e.m.

In addition, study by Larry J. Young showed that OXTR distribute densely in the MeA of prairie vole ⁶. This finding is consistent with our result that approximately 34% of neurons in the MeA were OXTR positive neurons marked by OXTR antibody (**Fig. 2e in manuscript**). Thus, the result that OXTR distribute extensively in the MeA is convincing.

5. Figure 2a-e: if the antibody works well, it is not clear why the OXTR is labeled using AAV-OXTR-mCherry. Based on Figure S3, the virus seems to only label a small fraction of OXTR cells. Thus, this strategy does not capture OXTR expression accurately. Why not just use the OXTR antibody?

Response: We appreciate your comment. Instead of AAV-OXTR-mCherry, the OXTR antibody was used to label OXTR cells in the revised manuscript (**Fig. 2a ~ e in manuscript**). In addition, instead of CTBs, the AAVs (2/R) were used to trace the MeA^{AI} and MeA^{VMHvl} to rule out the false-positive results. Results showed that the MeA^{OXTR+AI} and MeA^{OXTR+VMHvl} populations are largely separated in morphological distribution. Corresponding results text was showed in **pages 8, line 197-204**; Corresponding methods text was showed in **pages 32, line 771-776**.

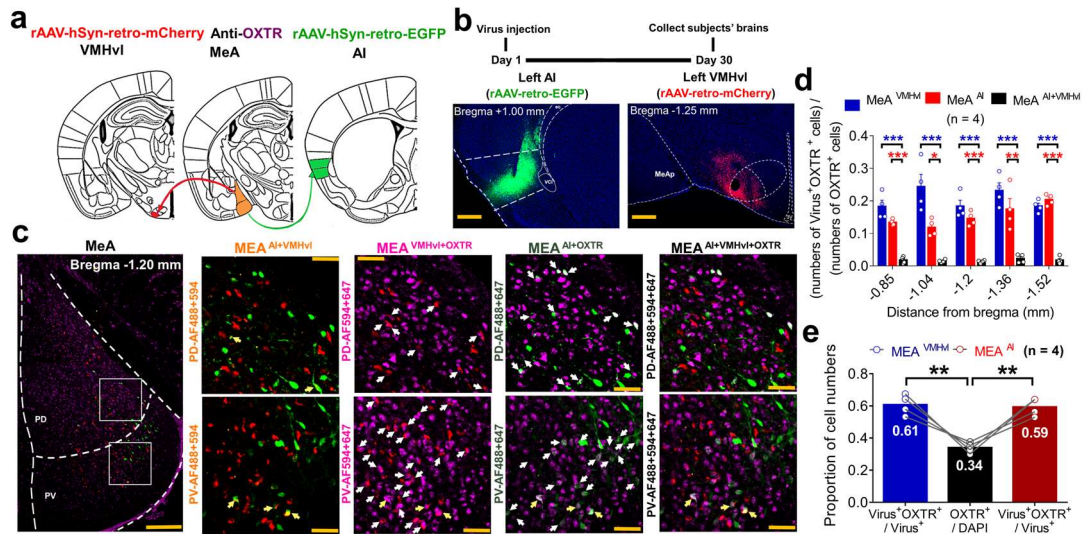


Fig. 2a ~ e in manuscript Distribution of the MeA^{OXTR+AI} and MeA^{OXTR+VMHvl}. (a and b) Diagram showing virus injection regimen (a) and schedule (b up); representative images of rAAV-retro-mCherry (red) and rAAV-retro-EGFP (green) injections sites at the VMHvl and AI, respectively (b down). scale bars, 500 μ m. (c) Representative overlapped images of dual-retrograde AAVs tracing and OXTR (magenta) at the both PD and PV subregions (left). The enlarged views of the selected white boxed areas (300 μ m \times 300 μ m, right). scale bars, 200 μ m (left) and 50 μ m (right). Merged neurons (MeA^{AI+VMHvl} and MeA^{AI+OXTR+VMHvl}) were characterized by yellow arrows. (d) The proportion of different retrograde virus positive and overlapped neurons expressing OXTR along the anteroposterior axis of the MeA. (e) Quantitative distinction between the proportion of different virus+ cells expressing OXTR and of the OXTR+ cells in the total MeA cells. $n = 4$ voles in (d ~ e). *** $p < 0.001$, ** $p < 0.01$, * $p < 0.05$; All error bars = s.e.m.

6. Figure 2f-s: please confirm the cell death by examining OXTR staining in the MeA after Cap3 vs. GFP injection. The lack of EGFP expression in MeA could be due to cell death or failed virus expression.

Response: Thanks for your suggestion. The OXTR cell death was confirmed by staining of OXTR antibody (**Fig. S9 in manuscript**). Results showed that caspase3 strategy successfully killed the MeA OXTR neurons projecting to the AI / VMHvl. Corresponding results text was showed in **pages 8, line 224-226**; Corresponding methods text was showed in **pages 33, line 827-831**.

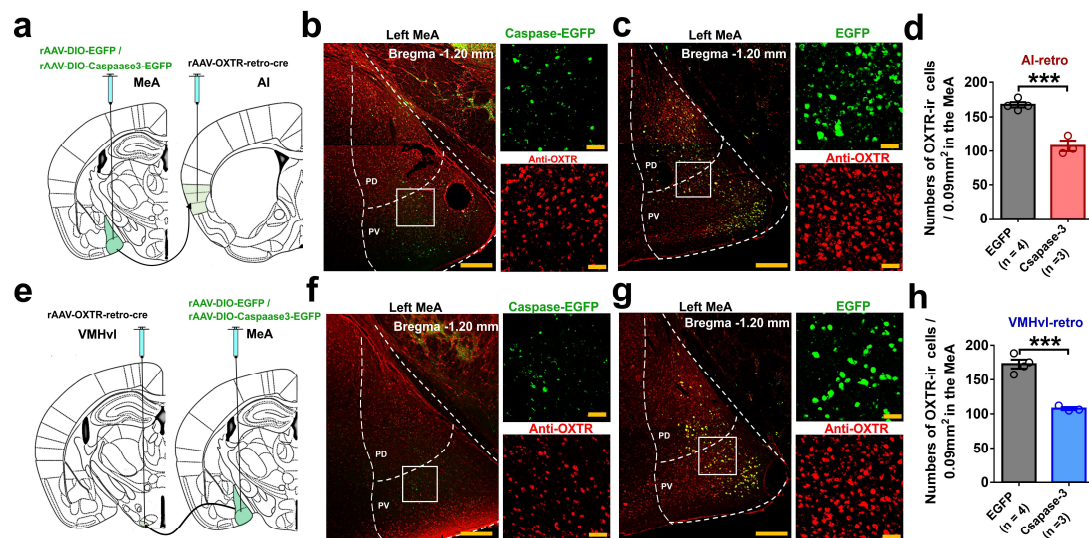


Fig. S9 in manuscript Confirming the cell death by examining anti-OXTR staining in the MeA after expression of AI / VMHvl-retro Caspase-3 virus in the MeA. (a and e) Diagram showing virus injection regimen. (b and c) Representative co-labeling images of AI-retro Caspase3 (b) or EGFP (c) (green) and corresponding anti-OXTR (red) in the MeA (left). The enlarged views of the selected white boxed areas (300 μ m \times 300 μ m, right). scale bars, 200 μ m (left) and 50 μ m (right). (d) Numbers distinction of OXTR-ir cells in the MeA between the AI-retro EGFP ($n = 4$ voles) and Caspase3 ($n = 3$ voles) groups. (f and g) Representative co-labeling images of VMHvl-retro Caspase3 (f) or EGFP (g) (green) and corresponding anti-OXTR (red) in the MeA (left). (h) Numbers distinction of OXTR-ir cells in the MeA between the VMHvl-retro EGFP ($n = 4$ voles) and Caspase3 ($n = 3$ voles) groups. *** $p < 0.001$, All error bars = s.e.m.

7. Figure 2f-2s, the clean behavior separation after killing MeA OXTR cells projecting to VMHvl vs. AI is surprising. Given that there is a substantial overlap between MeA cells projecting to VMHvl and AI. According to Figure 1c and 1d, 10% of MeA cells projecting to VMHvl and 7% projecting to both VMHvl and AI, meaning that MeA-AI cells include 70% of MeA-VMHvl cells. Thus, it is surprising that when MeA-AI cells are killed, which should also kill 70% of MeA-VMHvl cells, aggression does not change.

Response: Thanks a lot for your professional comments. According to **Fig. 2a ~ e and Fig. 1a ~ e in manuscript**, using AAVs (2/R) instead of CTBs to retrogradely trace neurons, the $MeA^{(OXTR+AI)}$ and $MeA^{(OXTR+VMHvl)}$ are largely separated from each other. Corresponding results text was showed in **pages 5, line 130-136**; Corresponding methods text was showed in **pages 30, line 710-714**. Such morphological separation indicated possible distinction in their functional roles. So the result that ablation of the $MeA^{OXTR+AI}$ did not change levels of aggression is acceptable now.

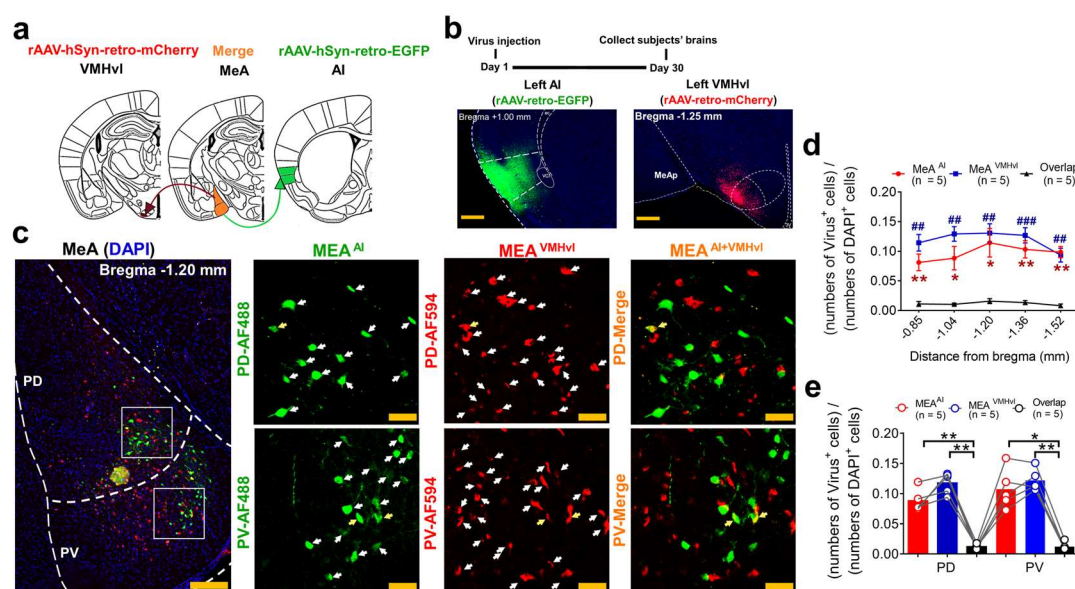


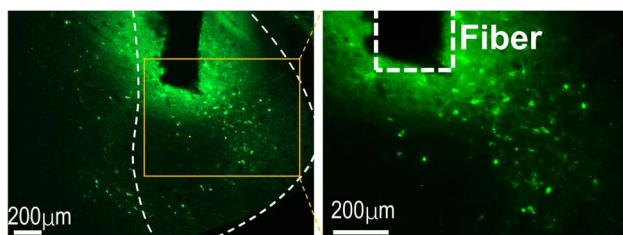
Fig. 1a ~ e in manuscript The distinct distribution of the MeA^{AI} and MeA^{VMHvl} . (a and b) Diagram showing virus (retrograde labeling) injection regimen (a) and schedule (b up); The representative images of rAAV-retro-mCherry (red) and rAAV-retro-EGFP (green) injections sites at the VMHvl and AI, respectively (b down). scale bars, 500 μ m. (c) Representative images with retro-virus labeling at the both posterior dorsal (PD) and posterior ventral (PV) subregions. The selected white boxed areas were enlarged (300 μ m \times 300 μ m, right). The $MeA^{AI+VMHvl}$ were characterized by yellow arrows. scale bars, 200 μ m (left) and 50 μ m (right). (d) The proportions of different virus positive and merged neurons at the MeA along the anteroposterior axis. * implies discrepancy between the Overlap and MeA AI. # implies discrepancy between the Overlap and MeA VMHvl. (e) The proportions of virus positive and overlapped neurons at the both PV and PD. $n = 5$ in (d and e). *** $p < 0.001$, ** $p < 0.01$. All error bars = s.e.m.

8. Figure 3d, e, n, o: the representative traces are of very different scales. Are the GCaMP6 signals of MeA OXTR-AI cells much weaker than that of MeA OXTR-VMHvl cells? If so, please explain especially given that there are more MeA cells projecting to AI than to the VMHvl.

Response: Thanks for pointing out this error and sorry for our carelessness. The scale of MeA OXTR-AI cells was incorrect as “2% $\Delta F/F$ ”. We have corrected it to “20% $\Delta F/F$ ” (**Fig. 3d and e in manuscript**). Intensities of GCaMP6 signals of MeA OXTR-AI cells and MeA OXTR-VMHvl cells were similar upon encountering shocked sibling or male intruder respectively.

9. Figure 3b and i: please indicate the optic fiber placement. Are the recordings from dorsal or ventral MeA? This is important considering that they are very different behavior functions.

Response: Thanks for your suggestion. The optic fiber placement was indicated in the figure of revised manuscript. As showed the follow representative image, the recordings are mainly from ventral MeAp.



10. Figure 3a-j: the lack of increase of MeA OXTR-Ai cells is again somewhat surprising given that AI projecting cells largely cover VMHvl projecting cells. Please discuss.

Response: Thank you for your rigorous consideration. According to **Fig. 2a ~ e and Fig. 1a ~ e in manuscript**, using AAVs (2/R) instead of CTBs to retrogradely trace neurons, the $\text{MeA}^{(\text{OXTR}^+)\text{AI}}$ and $\text{MeA}^{(\text{OXTR}^+)\text{VMHvl}}$ are largely separated from each other in the final version of our manuscript. The result that the activity of the $\text{MeA}^{(\text{OXTR}^+)\text{AI}}$ was increased while facing stressed siblings (but not meeting non-aggressive intruders) was acceptable now.

11. Figure 3: AUC analysis is not fair to all behaviors. For example, sniffing object episode is likely to be a lot shorter than 4s, thus 0-4s window will include periods that the behavior do not occur. The duration of the behavior episode should be taken into the consideration when analyzing the fiber photometry data.

Responses: Sorry for the confusing. To address your confusing, durations of all social behaviors were scored and averaged. It was found that duration of sniffing (stressed sibling, intruder or objects) was about 2 seconds. The post-phase duration was set as 2 seconds in AUC analysis. Mean duration of consolation was about 3.02 seconds and post-phase duration in in AUC analysis was set as 3 seconds. The aggression often contained 3 bouts of 1.1 seconds attacking and post-phase duration in AUC analysis was set as 3 seconds. The post-phase duration in AUC analysis was selected based on the duration of a specific behavior bout. Pre-phase durations of AUC were totally set as 2s. According above setting of post-phase duration in in AUC analysis, data of calcium signals in specific behavior were reanalyzed. Corresponding methods text was showed in **pages 35, line 903-907**. The result showed that calcium signals in the MeA^{OXTR+Al} were intensified upon sniffing or consoling siblings. In contrary, calcium signals in the MeA^{OXTR+VMHvl} were intensified upon sniffing or attacking intruders (**Fig. 3 in manuscript**). This result is consistent with that in original manuscript.

12. Figure S7: again, it is not clear why AAV-OXTR-mCherry is used instead of antibody. The antibody staining will be more straightforward and comprehensive. The number of virus infected cells is low. All figures should be better labeled to indicate what each color represents. Response: Thanks for your suggestion. The OXTR cells were marked using OXTR antibody instead of AAV-OXTR-mCherry virus in the revised manuscript (Fig. S16 in manuscript). Corresponding methods text was showed in pages 32, line 795-797 and line 806-809; Corresponding results text was showed in pages 13, line 316-318 and line 320-327. What each color represented was also labeled in all figures. No matter in PD or PV, numbers of the MeA^{OXTR+AI} activated by consolation and numbers of MeA^{OXTR+VMHvl} activated by aggression were more than controls.

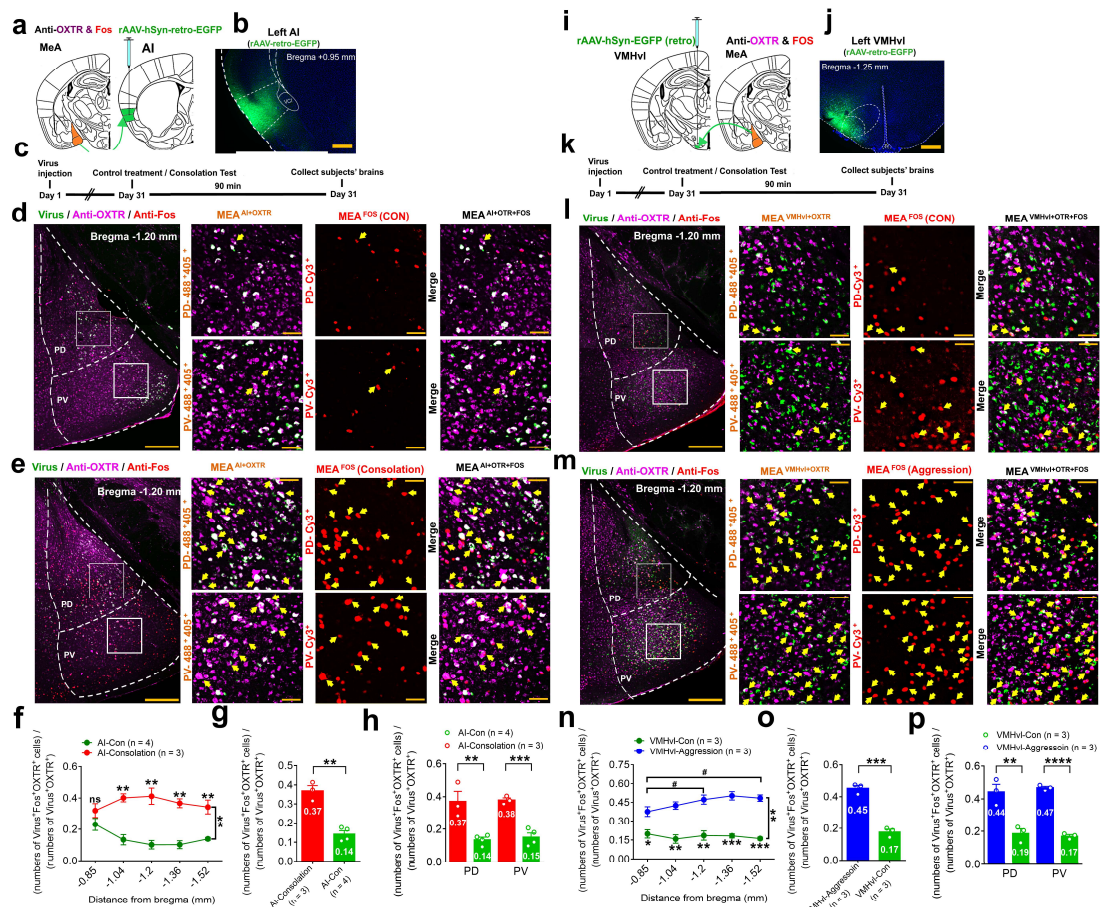


Fig. S16 in manuscript Morphological analysis of correlation between the MeA^{OXTR+AI} and consolation behavior, and between the MeA^{OXTR+VMHvl} and aggression. (a and c) and (i and k) Diagram showing retrograde AAVs injection regimen (a and i, left) and schedule (c and k). (b) and (j) Representative images of rAAV-retro EGFP (green) injections sites at the AI (b) and VMHvl (j). scale bars, 500 μ m. (d and e) and (l and m) Representative co-labeling images of AAVs tracing (green), anti OXTR (AF405, magenta) and anti c-Fos (Cy3, red) at the both PD and PV subregions after control treatment (d) and consolation test (e), or after control treatment (l) and resident-intruder paradigm (m), respectively. The enlarged views of the selected white boxed areas (300 μ m \times 300 μ m, right). scale bars, 200 μ m (left) and 50 μ m (right). Merged neurons (MeA^{AI+OXTR+c-Fos} and MeA^{VMHvl+OXTR+c-Fos}) were characterized by yellow arrows. (f) and (n) Proportion of activated neurons in the total OXTR neurons retrograded from the AI (f) and VMHvl (n), along the anteroposterior axis of the MeA (Green line: control treatment; red line: Consolation test; blue line: resident-intruder paradigm). * implies between-group discrepancy at a same site. # implies intergroup discrepancy at different sites. (g) and (o) Proportion distinction of activated OXTR neurons retrograded from the AI

between the Con and Consolation groups (g), or from the VMHvl between the Con and Aggression groups (o). (h) and (p) Proportion distinction of the triple-marked neurons in the both PD and PV subregions after the control treatment and consolation test (h), or after the control treatment and resident-intruder paradigm (p). In (f ~ h), AI-Con ($n = 4$ voles) and AI-Consolation ($n = 3$ voles) represented the proportion of MeA^{OXTR+AI+c-Fos} after the control and consolation, respectively. In (n ~ p), VMHvl-Con ($n = 3$ voles) and VMHvl-Aggression ($n = 3$ voles) represented percentage of MeA^{OXTR+VMHvl+c-Fos} after the control and resident-intruder paradigm, respectively. **** $p < 0.0001$, *** $p < 0.001$, ** $p < 0.01$, * $p < 0.05$; # $p < 0.05$. All error bars = s.e.m.

13. Figure 5: It is surprising that MeA OXTR cells that project to VMHvl and AI are primarily glutamatergic as MeA, especially its dorsal region, contains mainly GABAergic cells. MeA GABAergic cells but not glutamatergic cells promote inter-male aggression. The signal of antibody staining in Figure 5a is hardly convincing. In the text, it claims that Figure 5a and 5c show both Vglut2 and GABA staining, but only Vglut2 staining should be found in the figure. Please quantify the GABAergic vs. glutamatergic cells in the vole MeA as there might be species difference. Antibody often does not work as it should. It is important to validate the antibody. The authors may also consider using in situ hybridization to validate the neurotransmitter type of the cells.

Response: Thanks for your suggestion. To better clarify the main types of the two populations, the Gi-mCherry-MeA^{OXTR+AI} and Gi-mCherry-MeA^{OXTR+VMHvl} neurons were labeled by both anti-vesicular glutamate transporters (VGLut2) and anti-GABA (**Fig. 6a ~ d in manuscript**). Approximately 73.31% of the MeA^{OXTR+AI} neurons and 78.34% of the MeA^{OXTR+VMHvl} neurons were glutamatergic. Only 20.81% of the MeA^{OXTR+AI} neurons and 24.34% of the MeA^{OXTR+VMHvl} neurons were GABAergic. Electrophysiological data also revealed that main types of these two populations of neurons were glutamatergic (**Fig. 6e ~ k in manuscript**).

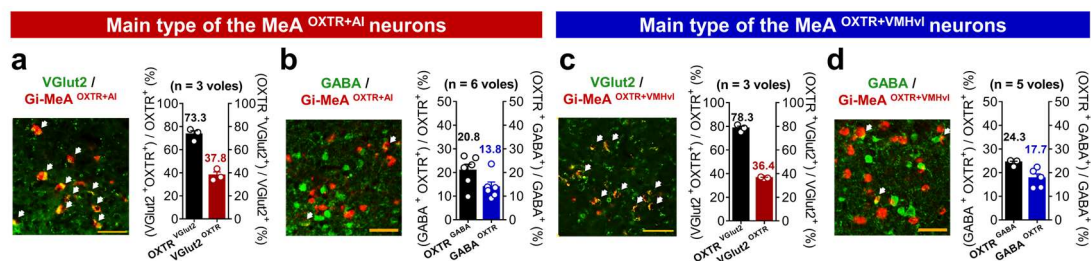
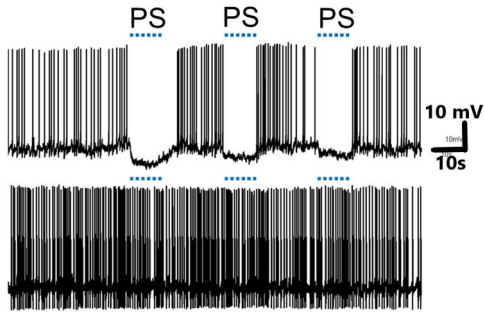


Fig. 6a ~ d in manuscript Representative overlapped images of hM4Di (Gi) and VGLut2, and Gi and GABA in the MeA^{OXTR+AI} (left parts of a and b) and MeA^{OXTR+VMHvl} (left parts of c and d), scale bars, 50 μ m. Quantification of the percentage of VGLut2 (GABA)-expressing Gi neurons and Gi-expressing VGLut2 (GABA) neurons in the MeA^{OXTR+AI} (right parts of a and b) and MeA^{OXTR+VMHvl} (right parts of c and d). $n = 3$ voles in (a) and (c). $n = 6$ in (b), and 5 in (d). All error bars = s.e.m.

14. Figure 5h-k, is there any monosynaptic IPSC evoked by the light?

Response: Thank you very much for your careful checking. In recording spontaneous discharge rate of AI neurons receiving projections from the MeA^{OXTR}, only one neuron showed inhibitory effect as the follow figure.



And this data has been integrated in the revised manuscript (**Fig. 6f in manuscript**); Corresponding methods text was showed in **pages 21, line 459**. Spontaneous discharge rates of AI and VMHvl neurons receiving monosynaptic anterograde projections from the MeA were recorded and it is confirmed that the MeA^{OXTR+AI} and MeA^{OXTR+VMHvl} exerted activating effects through glutamatergic mechanism (**Fig. 6f and g in manuscript**). In the following recording of postsynaptic potential in the AI and VMHvl, we mainly investigated type of glutamatergic receptors through which MeA^{OXTR+AI} and MeA^{OXTR+VMHvl} exerted their effects. We investigated whether infusion of two types of glutamate receptor antagonist, AP-5 or CNQX, could block oEPSC. We did not pay attention to and record oIPSC.

15. Given that MeA OXTR-AI and MeA Tac1/GABA-MPOA activation generates very similar behavior phenotype, the authors need to address whether these two are largely overlapping or distinct. Please consider perform dual retrograde labeling from AI and MPOA and examine the extent of overlap at MeA. Or examine the overlap between Tac1/GABA and MeA OXTR-AI cells.

Response: According to your suggestion, we investigated whether GABA and MeA^{OXTR+AI} were overlapped. According to **Fig. 6b and d in manuscript**, it is found that only 20.81% of the MeA^{OXTR+AI} neurons are labeled by GABA antibody. Combined with the conclusion that MeA^{Tac1+MPOA} is mainly GABAergic, the two populations should be morphologically distinct in the MeA. They may produce the similar behavioral effects through glutaminergic and GABAergic mechanism, respectively. We've also made a specific discussion in the revised manuscript (**Pages 26, line 567-575**).

16. The reviewer suggest the authors to remove the detailed stats in the main text as it makes the paper hard to read.

Response: Thanks for your suggestion. To make our article concise, clear and readable, detailed stats and source data in the main text have been moved to the supplementary files.

Extended data of the gene sequence of OXTR in mandarin voles:

>Oxtr

```
ATGGAGGGGCACCCCCGCAGCCAACTGGAGCTTCGAGTTGGACCTCGGGAGTGGCGTGTCTG
CCGGGGGTGGAGGGGAACCTCACAGCCGGGCCACCGCAGCGCAACGAGGCCCTGGCACGC
GTGGAGGTGGCGGTGCTGTGCCTCATTCTGTTCTGGCGCTGAGCGGCAACGCGTGCCTG
CTGCTGGCGCTGCGCACACACGCCACAAGCACTCGCGCTCTTCTTTTTCATGAAGCAC
CTGAGCATCGCCGACCTGGTGGTGGCTGTGTTCCAGGTGCTCCCGCAGCTGCTGTGGGAC
ATCACCTTCCGCTTCTACGGGCCGACCTGCTGTGCTGCTGCTGCAAGTACTTGCAGGTG
GTGGGCATGTTTCGCTTCCACCTACCTGCTGCTGCTTATGTCGCTCGACCGCTGCCTGGCC
ATCTGCCAGCCGCTGCGCTCTCTGCGACGCCGAACCGACCGCCTGGCGGTGCTAGCAACA
TGGCTGGGCTGCCTGGTGGCCAGCGCGCCGAGGTGCACATTTTCTCGCTGCGCGAAGTG
GCGGACGGTGTGTTTTGACTGCTGGGCTGTCTTCATCCAGCCTTGGGGACCCAAGGCCTAC
GTCACCTGGATCACACTTGCCGTCTACATTGTTCCCGTCATAGTGCTGGCCGCGCTGCTAT
GGCCTCATCAGCTTCAAGATCTGGCAGAACCTGCGACTCAAGACGGCAGCGGCGGCGGCC
GAGGGGACTGAGGGATCTGCTGCCGGTGGAGCTGGGCGCGCGGCGCTGGCTCGGGTCACT
AGCGTCAAGCTCATCTCCAAGGCCAAGATCCGCACAGTGAAAATGACCTTCATCATTGTA
CTGGCCTTCATCGTGTGCTGGACGCCTTCTTCTTCGTGCAGATGTGGAGCGTCTGGGAC
GTCAATGCACCCAAGGAAGCTTCTGCCTTCATCATCGCCATGCTCTTGGCCAGCCTCAAC
AGCTGCTGCAACCCCTGGATCTACATGCTGTTACGGGCCACCTCTTTCACGAACCTTGTG
CAGCGCTTCTCTGCTGCTCTGCCGCTACCTGAAGGGCAGCAGGCCCGGAGAGACGAGT
GTCAGCAAGAAAAGCAACTCGTCCACCTTCGTCTGAGTCGCCGAGCTCCAGCCAGAGG
AGCTGCTCTCAGCCCTCTTCCGCATGA
```

1. Zingg B, *et al.* AAV-Mediated Anterograde Transsynaptic Tagging: Mapping Corticocollicular Input-Defined Neural Pathways for Defense Behaviors. *Neuron* **93**, 33-47 (2017).
2. Tervo DG, *et al.* A Designer AAV Variant Permits Efficient Retrograde Access to Projection Neurons. *Neuron* **92**, 372-382 (2016).
3. Mei L, Yan R, Yin L, Sullivan RM, Lin D. Antagonistic circuits mediating infanticide and maternal care in female mice. *Nature* **618**, 1006-1016 (2023).
4. Qi G, *et al.* NAc-VTA circuit underlies emotional stress-induced anxiety-like behavior in the three-chamber vicarious social defeat stress mouse model. *Nat Commun* **13**, 577 (2022).
5. Tsai NY, *et al.* Trans-Seq maps a selective mammalian retinotectal synapse instructed by Nephronectin. *Nat Neurosci* **25**, 659-674 (2022).
6. Inoue K, Ford CL, Horie K, Young LJ. Oxytocin receptors are widely distributed in the prairie vole (*Microtus ochrogaster*) brain: Relation to social behavior, genetic polymorphisms, and the dopamine system. *J Comp Neurol* **530**, 2881-2900 (2022).

Point-to-point responses:

(Reviewers' comments in Blue; Our responses in Black)

PS: All changes in the revised manuscript text file are marked with red underline.

Reviewer #3 (Remarks to the Author):

This study focuses on understanding the circuit mechanisms that control the switch between consolation and aggression in highly social mandarin voles. The authors identified two distinct subtypes of oxytocin receptor (OXTR) neurons in the medial amygdala (MeA) that project to the anterior insula (AI) and ventromedial hypothalamus (VMHvl). These neurons respond differently to stressed siblings or unfamiliar intruders. By manipulating these pathways, the researchers observed altered responses to social stimuli. The main type of glutamate receptors involved in these pathways is AMPA receptors in the AI and VMHvl. These findings suggest that the two subtypes of OXTR neurons in the MeA play a crucial role in controlling consolation and aggression. Although this work is potentially interesting, its conceptual advance is limited, and the major conclusions are not convincingly supported by the data. There are a number of major issues concerning the main findings:

Response: Thanks for your comments and suggestions. These suggestions are helpful and valuable for improving our works. We made response to your comments one by one as following.

Comment 1. There is no causal evidence showing if OXTR neurons are specifically involved in consolation and aggression or if they simply reflect a random subset of neurons that can promote these behaviors. Indeed, previous studies have shown that tachykinin neurons in the MeA mediate consolation and tachykinin-negative neurons mediate aggression (Wu et al 2021). This suggests that OXTR neurons are likely not a specific population for these behaviors.

Response: Thanks for your valuable suggestion.

1) Using (fluorescence in situ hybridization, FISH) method (**Fig. S6 in manuscript**), it is found that neurons marked by OXTR mRNA fluorescence probe were completely overlapped with neurons stained by OXTR antibody. It is suggested that staining via OXTR antibody is specific to OXTR cells. Corresponding results text was indicated in **pages 8, line 194-196**; Corresponding methods text was showed in **pages 31, line 757- pages 32, line 770**. Using apoptosis to respectively kill the MeA OXTR neurons projecting to AI and VMHvl, or optogenetic and pharmacogenetic manipulation of these two populations of somata / fibers specifically affect consolation and aggression respectively. It is suggested that MeA OXTR neurons projecting to AI and VMHvl causally and specifically regulate consolation and aggression behaviors respectively.

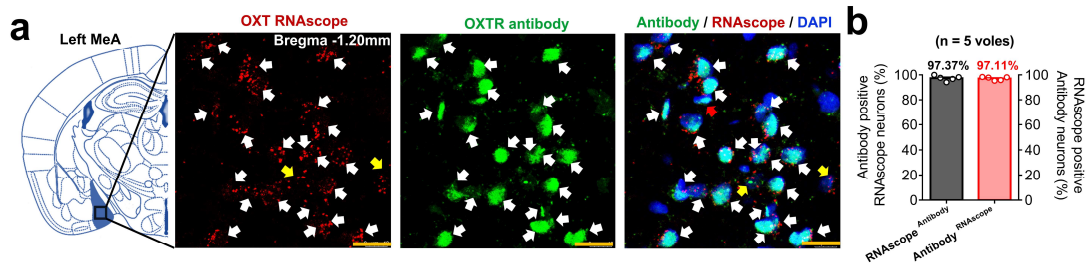


Fig. S6 in manuscript The validation of the efficiency and accuracy of OXTR antibody by RNAscope Multiplex Fluorescent v2 Assay combined with Immunofluorescence-Integrated Co-detection Workflow (ICW). (a) Representative co-labeling images of OXTR RNAscope (AF570, red) and OXTR antibody (AF488, green). Co-labeling neurons were characterized by white arrows. The neurons labeled by antibody but not RNAscope were characterized by red arrows. The neurons labeled by RNAscope but not antibody were characterized by yellow arrows. scale bars, 15 μ m. (b) The percentage of co-labeling neurons in antibody positive neurons and in RNAscope positive neurons, respectively ($n = 5$ voles). All error bars = s.e.m.

2) According to study by Hong group (Wu et al 2021), the MeA Tac1 neurons projecting to MPOA (MeA^{Tac1+MPOA}) is mainly GABAergic¹. However, according to results of the present study (**Fig.6 a ~ d in manuscript**), the MeA OXTR neurons projecting to AI (MeA^{OXTR+AI}) neurons are mainly glutaminergic (about 80%). And electrophysiological data also confirmed this result (**Fig.6 e ~ k in manuscript**). The MeA^{Tac1+MPOA} and MeA^{OXTR+AI} neurons may be morphologically distinct in the MeA. They may generate the similar behavioral performance through glutaminergic and GABAergic mechanism, respectively. We've also addressed this in the discussion (**Pages 26, line 567-575**).

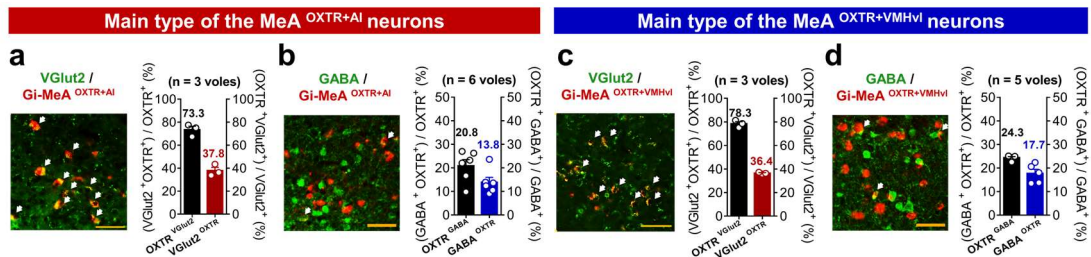


Fig.6 a ~ d in manuscript Representative overlapped images of hm4Di (Gi) and VGlut2, and Gi and GABA in the MeA^{OXTR+AI} (left parts of a and b) and MeA^{OXTR+VMHvl} (left parts of c and d). scale bars, 50 μ m. Quantification of the percentage of VGlut2 (GABA)-expressing Gi neurons and Gi-expressing VGlut2 (GABA) neurons in the MeA^{OXTR+AI} (right parts of a and b) and MeA^{OXTR+VMHvl} (right parts of c and d). $n = 3$ voles in (a) and (c). $n = 6$ in (b), and 5 in (d). All error bars = s.e.m.

3) Honestly, we thought there is limitation in our previous study. Only involvements of MeA OXTR neurons in consolation and aggression were investigated. Whether levels of OXT release in the MeA and activities of PVN OXT neurons projecting to MeA were altered upon consoling or attacking remains unclear. Answering this question can add evidence to our finding that MeA OXTR neurons causally regulate consolation and aggression, but not just overlapped with a random subset of neurons that can promote these behaviors. In the following experiments, new oxytocin sensor1.0 developed by Yulong Li lab² was used to measure OXT release in the MeA upon consoling and attacking. Changes in calcium signal of PVN OXT neurons projecting to MeA were also detected. The result showed that MeA

OXT release and activities of PVN OXT neurons projecting to MeA were significantly increased upon consoling and attacking displaying the strong involvement of OXT system at the MeA in occurrence of consolation and aggression (Fig. S11 in manuscript, corresponding methods text was showed in pages 12, line 263-285; Corresponding results text was showed in pages 34, line 846-863). Combined with result of genetic manipulation (Fig. 4 ~ 5 and Fig. 6l ~ z in manuscript), we are convinced that MeA OXTR neurons projecting to AI and VMHvl regulate consolation and aggression respectively mainly via a glutaminergic mechanism.

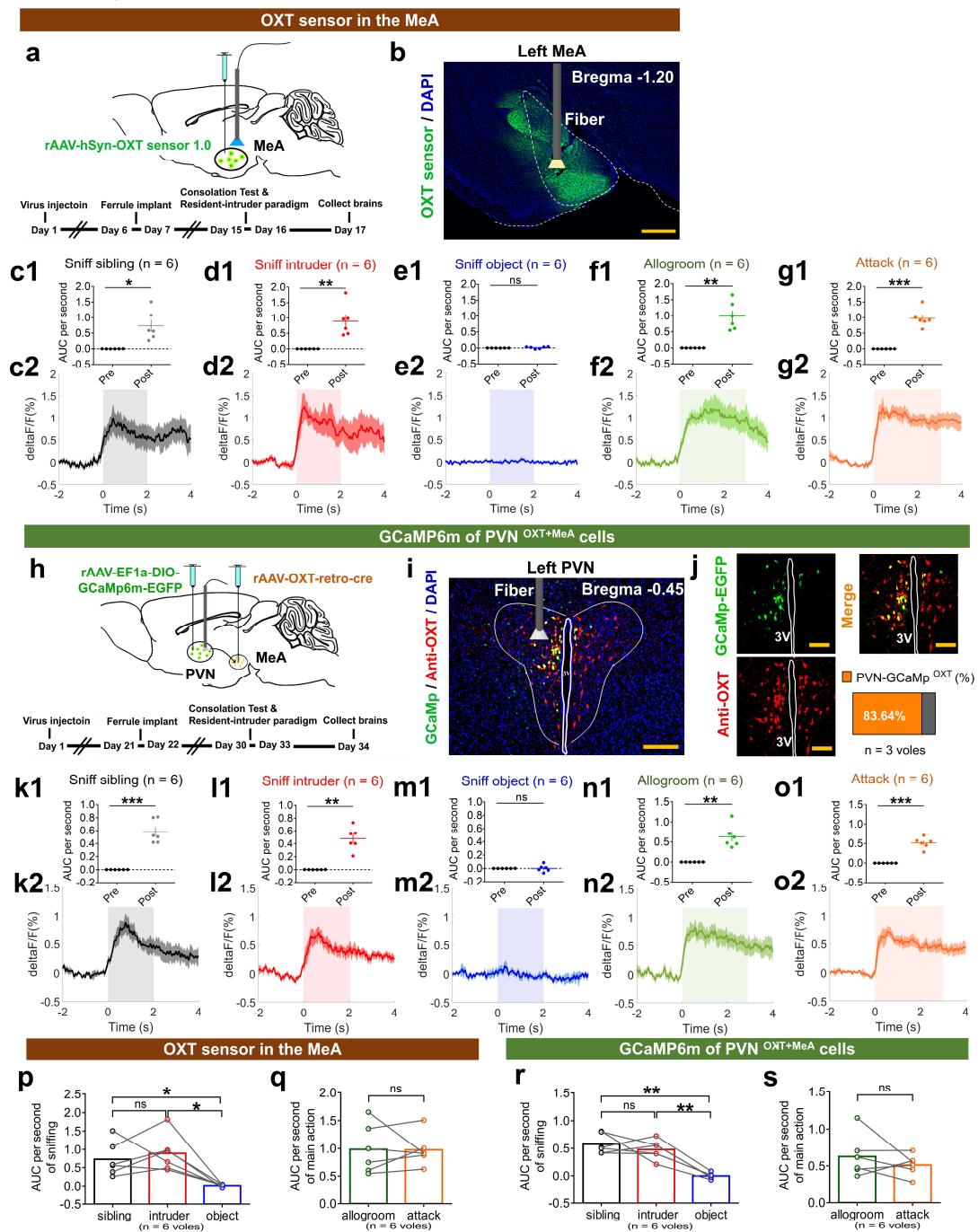


Fig. S11 in manuscript Changes in fluorescence signals in the MeA^{OXT sensor} and PVN^{OXT+MeA} during various social behaviors. (a) and (h) Virus regimen (up) and schedule (down) for fluorescent signal recording of the MeA^{OXT sensor} (a) and PVN^{OXT+MeA} (h). (b) and (i) Images of OXT sensor and GCaMP6m (green) expression in the MeA (b) and PVN^{OXT+MeA} (i). scale bars,

500 μm (b) and 200 μm (i). (j) Overlapped images of OXT-GCaMp6m (green) and anti-OXT (red). scale bars, 100 μm ; Statistical charts showed the MeA-retro OXT-GCaMp6m positive neurons were relatively restricted to anti-OXT cells (j down right). Three voles were used in (j). (c1 ~ g1) Changes of fluorescent signals in the MeA^{OXT sensor} before and after sniffing siblings (c1), sniffing intruder (d1), sniffing object (e1), allogrooming (f1) and attacking (g1). (c2 ~ g2) Peri-event plot of the representative signal ($\Delta F/F$, %) in the MeA^{OXT sensor} aligned to onsets of various social behaviors (the colored line is the averaged signal trace, whereas the corresponding shaded region denotes the s.e.m.). (k1 ~ o1) Changes of calcium signals in the PVN^{OXT+MeA} before and after sniffing siblings (k1), sniffing intruder (l1), sniffing object (m1), allogrooming (n1) and attacking (o1). (k2 ~ o2) Peri-event plot of the representative calcium signal in the PVN^{OXT+MeA} aligned to onsets of various behaviors. (p ~ s) AUC per second distinctions of fluorescent signal traces during different social behaviors in the MeA^{OXT sensor} (p and q) and PVN^{OXT+MeA} (r and s). Six voles' calcium signals were collected in the MeA^{OXT sensor} (c1 ~ g2, p and q). Six voles' calcium signals were collected in the PVN^{OXT+MeA} (k1 ~ o2, r and s); ***p < 0.001, **p < 0.01, *p < 0.05. All error bars = s.e.m.

2. The authors need to validate the viral tools used for retrograde labeling in mandarin voles and to make sure that AAV (retro) indeed labels neurons in a retrograde manner. Although these tools are known to work well in mice, they may not work in the same manner in mandarin voles. Previous studies show that viral vectors work very differently across species. The authors also need to rule out the possibility that this AAV (retro) may label neurons in an anterograde manner (anterograde transsynaptic labeling). The cells labeled in Figure 1i and 1j look very broad and non-specific.

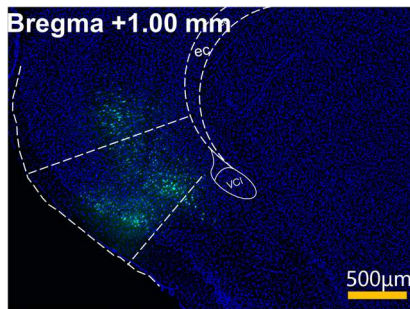
Response:

1) ① Viral vectors are by far the best option to retrogradely trace upstream neurons through entering axonal terminals and retrograde transport of their payload to the cell nuclei. In 2016, a newly evolved variant, rAAV2/R, was developed by researchers³. The rAAV2-retro gene delivery system can be used on its own or in conjunction with Cre recombinase driver lines to effectively investigate function of neural circuit, as well as for genome editing in targeted neuronal populations⁴. Up to now, the rAAV2-Retro vector, as a powerful tool for investigation of neuronal circuit, has been used in number of species with distant relatedness⁵, such as rat^{6, 7, 8}, nonhuman primate (rhesus macaque⁹ and Cynomolgus Macaque⁵) and mandarin voles^{10, 11} in addition to mice. This indicates that property of rAAVs (2/R) in retrograde tracing of neuronal circuit across different species is widely recognized.

② In mandarin voles, rAAVs (2/R) have been used to investigate neural circuits underlying paternal care / infanticide (DR-MPOA and PVN-VTA)^{10, 11}, consolation (DR-ACC)¹², and disorders in emotion and social behaviors induced by social defeat (PVN-NAc)¹³. These studies have been published in eLife and Journal of Neuroscience ect. We agree with your opinion that retrograde tracing of AAVs (2/R) in mandarin voles may be not very strict and further elaborating investigation on this point using new experiment would be helpful. However, AAVs (2/R) combined with cre-DIO system used in the present study may be one of the most effective strategies to trace specific circuits.

2) In the Fig.1i and 1 of original version, all neurons in the MeA that project to AI, but not limited to the MeA OXTR neurons projecting to AI, were labeled. Thus, the cells labeled in Figure 1i and 1j look relatively broad. In addition, we provided a representative EGFP image in lower magnification ($\times 4$) that showed specific expressions in injection sites as

follows.



In order to further exclude confounding of using AAV1 as anterograde tracer on experimental results, rAAV-CAG-mWGA-mCherry that can strictly and anterogradely travel across single synapse was injected into the MeA (**Fig. S5 in manuscript**)¹⁴, the neurons that co-labeling mCherry tracer and c-Fos in the AI and VMHvl were counted after consolation or aggression. Unpaired T-test analysis revealed that the activities of neuron in the AI and VMHvl that receive projections from MeA during Control, consolation and aggression did not show significant difference between two strategies using AAV1 and CAG-mWGA as anterograde tracer (**Fig. S5k and l in manuscript**). Corresponding results text was showed in **pages 5, line 153-160**; Corresponding methods text was showed in **pages 31, line 746-756**.

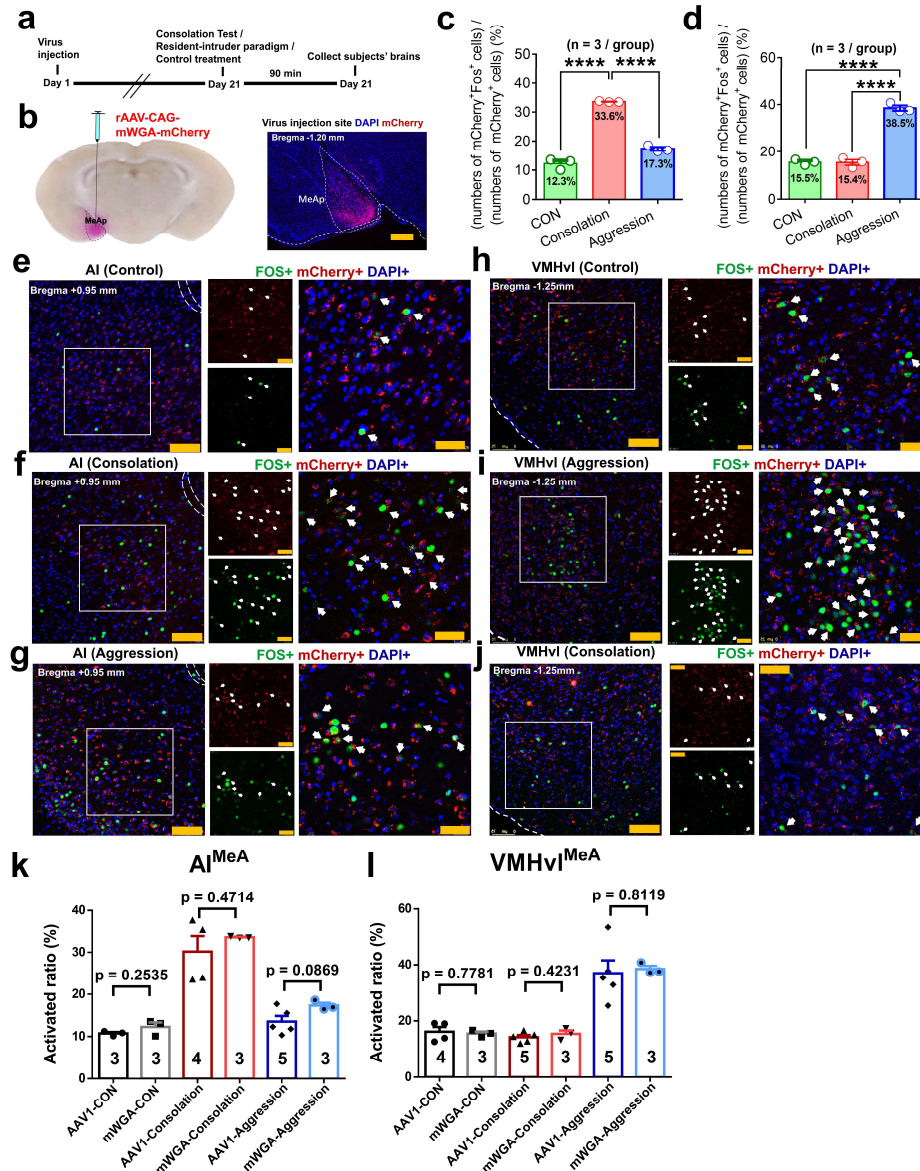


Fig. S5 in manuscript Using fluorescent anterograde trans-synaptic tracer (mWGA-mCherry) and c-Fos labeling to map post-synaptic (the AI and VMHvl) neuronal activity from the MeA during different behaviors. (a and b) Diagram showing injection schedule (up) and site (down) of anterograde monosynaptic labeling virus. (c) Comparison of percentage of mCherry and c-Fos co-labeling AI neurons in whole anterograde virus-marked neurons between the CON, Consolation and Aggression groups. (d) Comparison of percentage of mCherry and c-Fos co-labeling VMHvl neurons in whole anterograde virus-marked neurons between the CON, Consolation and Aggression groups. (e, f and g) Representative overlapped images of anterograde monosynaptic virus (red) and c-Fos (green) at the AI after control treatment (CON, $n = 3$ voles, e), consolation test (Consolation, $n = 3$ voles, f) and resident-intruder paradigm (Aggression, $n = 3$ voles, g). (h, i and j) Representative overlapped images of anterograde virus and c-Fos at the VMHvl after control treatment (CON, $n = 3$ voles, h), consolation test (Consolation, $n = 3$ voles, i) and resident-intruder paradigm (Aggression, $n = 3$ voles, j), respectively. The enlarged views of the selected white boxed areas ($300 \mu\text{m} \times 300 \mu\text{m}$, right), and co-labeling neurons were characterized by white arrows. scale bars, $100 \mu\text{m}$ (left) and $50 \mu\text{m}$ (right). (k) and (l) The distinction of co-labeled c-Fos and fluorescent tracer ratio between AAV (2/1) system and CAG-mWGA strategy in the AI^{MeA} (k) and VMHvl^{MeA} (l). **** $p < 0.0001$. All error bars = s.e.m.

Finally, Fos and EGFP co-labeled cells in the VMHvl and AI after both consolation and

aggression were quantified (**Fig. 1 l and m, and p and q in manuscript**). The result showed that neurons in the AI and VMHvl could be activated by consolation or aggression specifically. Corresponding results text was added in **pages 5, line 148 and 151-152**.

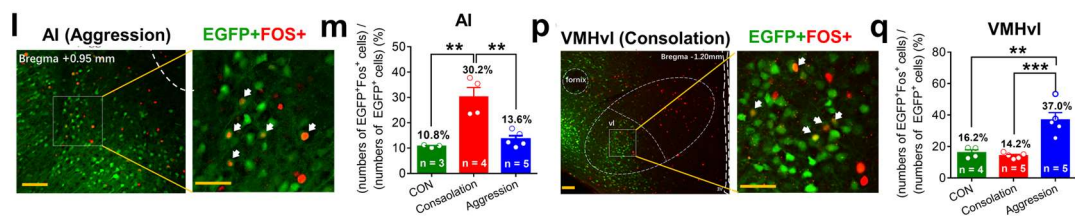


Fig. 1 l and m, and p and q in manuscript The percentage of EGFP and c-Fos co-labeled cells in the AI and the VMHvl under aggression or consolation. ***p < 0.001, **p < 0.01. All error bars = s.e.m.

3. Since Vglut2 is only expressed in a subset of Oxt neurons (Fig. 5b), it is unclear if Oxt neurons mediate consolation and aggression through a glutamatergic mechanism. The authors should confirm this by directly manipulating glutamatergic neurons in the MeA or glutamatergic Oxt neurons in the MeA.

Response: Thanks for your suggestion. To address this issue, the additional experiment was conducted. As showed in **Fig. 6l ~ z in the manuscript**, we directly activated fibers located in the AI or VMHvl of the glutamatergic MeA^{OXT^R} neurons, and corresponding results have been added in **pages 21, line 473-pages 22, line 489**. These results indicated that optogenetic activation of glutamatergic MeA^{OXT^R+AI} and MeA^{OXT^R+VMHvl} fibers were sufficient to increase consolation and aggression, respectively. Corresponding methods text was showed in **pages 36, line 927-938**.

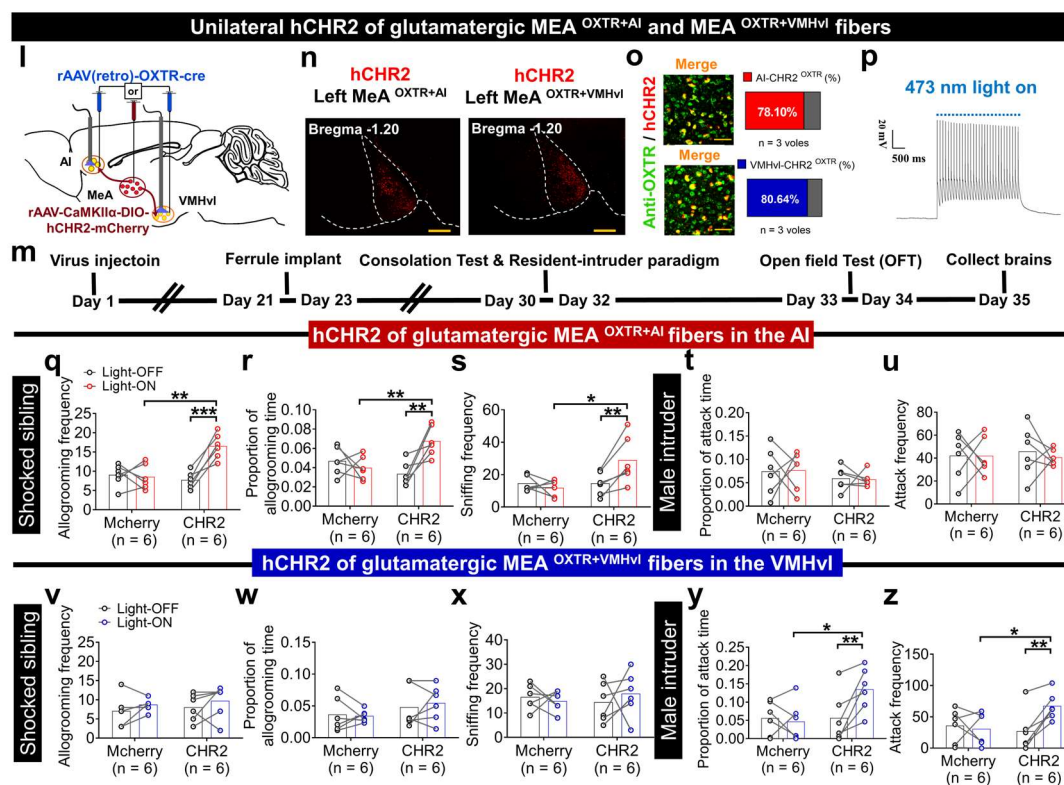


Fig. 6l ~ z in the manuscript (l) and (m) Virus regimen (l) and schedule (m) for optogenetic activation of the glutamatergic fibers of the MeA^{OXT^R+AI} and MeA^{OXT^R+VMHvl}. (n) Images of hChR2 expression (red). scale bars, 500 μ m. (o) Representative overlapped images of hChR2 and anti-OXTR. scale bars, 50 μ m; Statistical charts showed AI- and VMHvl-projecting hChR2 neurons were relatively restricted to anti-OXTR cells. $n = 3$ voles / group. (p) Representative electrophysiological traces showing photoactivation effect. (q ~ u, and v ~ z) Comparison of allogrooming (q, r, v and w) and sniffing siblings (s and x), and attacking intruders (t, u, y and z) between the hChR2 and mCherry groups in the MeA^{OXT^R+AI} and MeA^{OXT^R+VMHvl}. $n = 6$ voles in each group in (q ~ z). *** $p < 0.001$, ** $p < 0.01$, * $p < 0.05$. All error bars = s.e.m.

4. The authors performed optogenetic activation of MeA neuron terminals in the VMHvl and AI. However, they didn't show any behavioral phenotypes that are associated with these manipulations. To support the main conclusion of this study, it is essential to determine if optogenetic activation of MeA neuron terminals in the VMHvl and AI produces a similar behavioral phenotype.

Response: Thanks for your suggestion. As showed in **Fig. 4p ~ c'** in manuscript, we directly activated fibers located in the AI or VMHvl from the MeA^{OxTR} neurons, and corresponding results have been added in **pages 16, line 365-379**. The result we obtained via optogenetic activation of terminals in the VMHvl and AI is similar to the result by optogenetic activation of MeA neurons projecting to the VMHvl and AI.

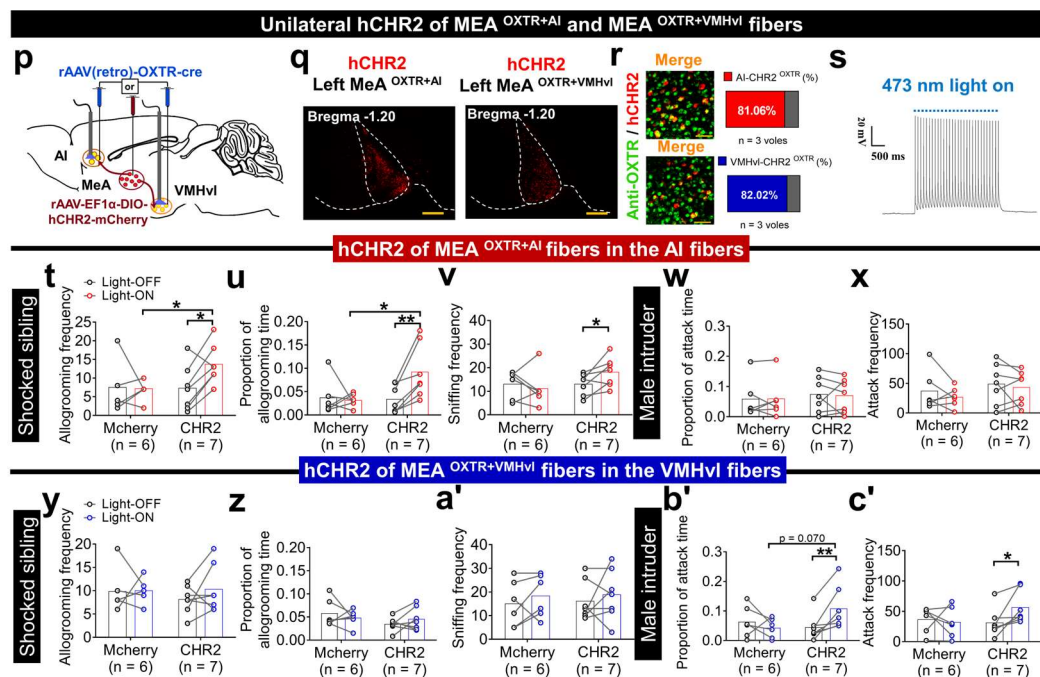


Fig. 4p ~ c' in manuscript Effects of optogenetic activation of fibers of the MeA^{OxTR+AI} and MeA^{OxTR+VMHvl} on consolation and aggression. (p) Virus regimen for optogenetic activation of fibers of the MeA^{OxTR+AI} and MeA^{OxTR+VMHvl}. (q) Images of OxTR-hChR2 expression (red) in the MeA^{OxTR+AI} and MeA^{OxTR+VMHvl}. scale bars, 500 μ m. (r) Overlapped images of OxTR-hChR2-mCherry (red) and anti-OxTR (AF488, green) in the MeA^{OxTR+AI} and MeA^{OxTR+VMHvl}. scale bars, 50 μ m; Statistical charts showed AI-projecting (r up right) and VMHvl-projecting (r down right) OxTR-hChR2 positive neurons were relatively restricted to OxTR cells. n = 3 voles / group for verifying specificity of OxTR-hChR2. (s) Representative traces from electrophysiological recordings showing photoactivation of the MeA^{OxTR+AI} or MeA^{OxTR+VMHvl} somata. (t ~ x) Comparison of allogrooming (t and u) and sniffing siblings (v), and of attacking intruders (w and x) between the AI-retro CHR2 and mCherry groups in activating fibers. n (mCherry) = 6 voles, n (CHR2) = 7 voles. (y ~ c') Comparison of allogrooming (y and z) and sniffing siblings (a'), and of attacking intruders (b' and c') between the VMHvl-retro CHR2 and mCherry groups in fibers. n (mCherry) = 6 voles, n (CHR2) = 7 voles in. **p < 0.01, *p < 0.05. All error bars = s.e.m.

5. The retrograde labeling from VMHvl and AI in the MeA labels neurons that may also project colaterally to other brain areas. The fact that activating retrogradely labeled cell bodies can promote a behavior does not necessarily mean that it is the MeA-VMHvl or MeA-AI projections that mediate these behavioral functions. The authors should perform experiments to rule out the involvement of other collateral projections of these two neuronal populations in consolation and aggression.

Response: Thanks for your suggestion. As showed in **Fig. 4p ~ c' and Fig. 6l ~ z in manuscript**, we directly activated fibers located in the AI or VMHvl from the (glutamatergic) MeA^{O_XTR} neurons. The optogenetic manipulation activates specific projections or glutamatergic projections and the results obtained are convincing. The two additional experiments ruled out the involvement of other collateral projections of these two neuronal populations in consolation and aggression.

6. The authors should express a fluorescent maker in MeA OXTR neurons, confirm if they can identify axonal terminals in VMHvl, AI and other brain regions such as the BNST and the preoptic area, and quantify the axon projection density of these neurons in these brain areas.

Response: Thanks for your consideration. The additional experiment was conducted. And results of this part were added in the revised manuscript (**Fig. S8 in manuscript**). No distinction of OXTR fibers' integrated optical density (IOD) was found between the AI and MPOA, or between the VMHvl and BNST. These results indicated that MeA OXTR neurons exhibited similar intensities of projections to these four downstream brain regions. Corresponding results text was showed in **pages 8, line 210-219**; Corresponding methods text was showed in **pages 32, line 784-792**.

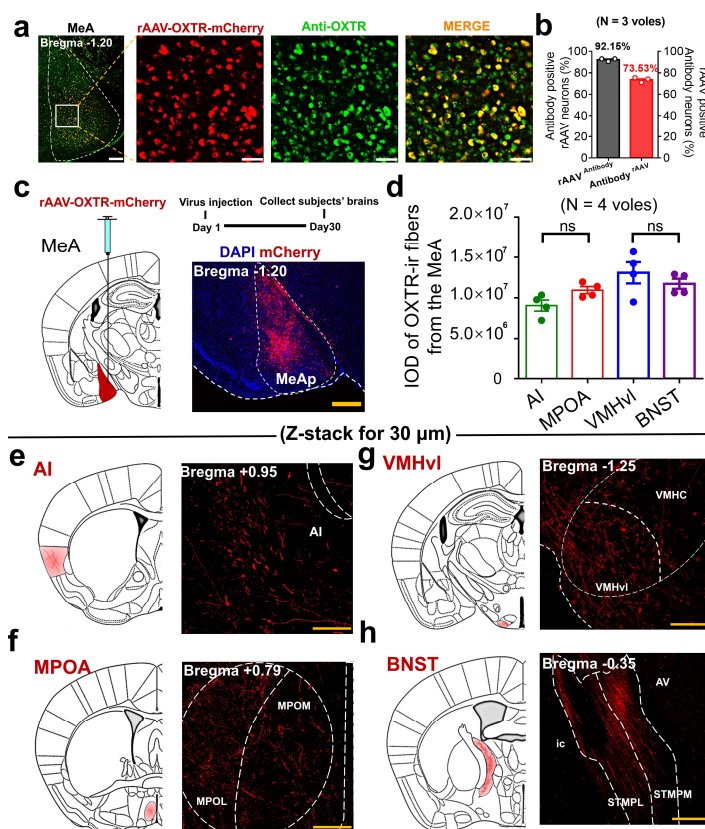


Fig. S8 in manuscript Quantification of density of OXTR-ir fibers in the AI, MPOA, VMHvl and BNST after verification of transfection efficiency of rAAV-OXTR-mCherry by OXTR antibody. (a) Overlapped images of neurons infected by rAAV-OXTR-mCherry (red) and neurons stained by OXTR antibody (green) (a left). The enlarged views of the selected white boxed areas (300 µm×300 µm) (a right). scale bars, 200 µm (left) and 50 µm (right). (b) Quantification of the percentage of antibody-staining infective OXTR-mCherry neurons and OXTR-mCherry expressing antibody-staining neurons. *N* = 3 voles. (c) Diagram showing virus injection regimen (left), schedule (up right) and representative images of rAAV injection site. scale bars, 500 µm. (d) Differences in IOD of OXTR-ir fibers between the AI, MPOA, VMHvl and BNST. *N* = 4 voles. (e ~ h) Representative 30µm Z-stack images of OXTR-ir fibers (red) in the AI (e), MPOA (f), VMHvl (g) and BNST (h). scale bars, 100 µm. All error bars = s.e.m.

7. The percentage of OXTR neurons shown in Fig. 2e seems to be substantially higher than what was shown in the representative images in Fig. 2b, particularly outside the boxes. This questions the validity of the quantification. The authors should also show more representative images from different areas of the MeA in higher magnification.

Response: Thanks. According to your valuable suggestion, the OXTR antibody, instead of rAAV-OXTR-mcherry was used to label OXTR positive cells to rule out the nonuniformity of virus expression in the MeA as mentioned in this comment. In addition, we used AAVs(2/R) instead of CTBs to retrogradely mark the MeA^{AI} and MeA^{VMHvl} to rule out the possible false-positive results by CTBs. As showed in **Fig. 2a ~ e in manuscript**, results indicated that the MeA^{OXTR+AI} and MeA^{OXTR+VMHvl} populations are largely distinct in morphological distribution. These results are more convincing. Corresponding results text was showed in **pages 8, line 197-204**; Corresponding methods text was showed in **pages 32, line 771-776**.

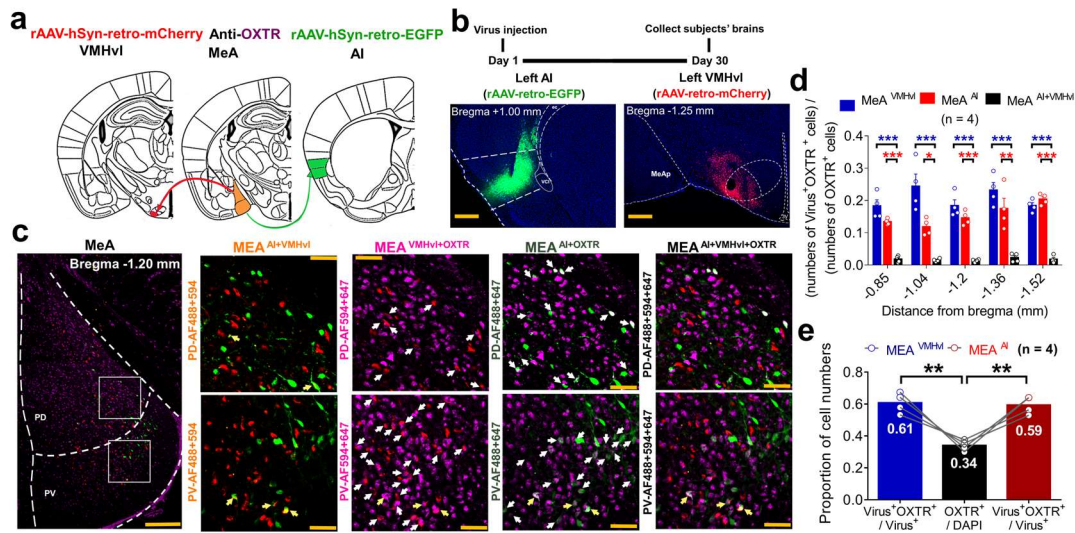


Fig. 2a ~ e in manuscript Distribution of the MeA^{OXTR+AI} and MeA^{OXTR+VMHvl}. (a and b) Diagram showing virus injection regimen (a) and schedule (b up); representative images of rAAV-retro-mCherry (red) and rAAV-retro-EGFP (green) injections sites at the VMHvl and AI, respectively (b down). scale bars, 500 μ m. (c) Representative overlapped images of dual-retrograde AAVs tracing and OXTR (magenta) at the both PD and PV subregions (left). The enlarged views of the selected white boxed areas (300 μ m \times 300 μ m, right). scale bars, 200 μ m (left) and 50 μ m (right). Merged neurons (MeA^{AI+VMHvl} and MeA^{AI+OXTR+VMHvl}) were characterized by yellow arrows. (d) The proportion of different retrograde virus positive and overlapped neurons expressing OXTR along the anteroposterior axis of the MeA. (e) Quantitative distinction between the proportion of different virus+ cells expressing OXTR and of the OXTR+ cells in the total MeA cells. $n = 4$ voles in (d ~ e). *** $p < 0.001$, ** $p < 0.01$, * $p < 0.05$; All error bars = s.e.m.

8. In light of the recent paper indicating that Oxt is not required for social attachment in voles (Berendzen et al 2023), it is important to perform additional experiments to examine and confirm the functional involvement of Oxt and the oxytocin signaling in these Oxt-expressing neurons during consolation and aggression.

Response: As reviewers suggested, some additional experiments have been performed.

1) As result showed in **Fig. 6l ~ z and Fig. 4p ~ c' in manuscript**, optogenetic activation of (glutamatergic) MeA OXTR neurons' terminals in the VMHvl and AI specifically increased aggression and consolation respectively. This result was similar to that of optogenetic activation of MeA neurons with specific projections.

2) As result showed in **Fig. S11 in manuscript**, OXT release in the MeA and activities of PVN OXT neurons projecting to MeA were increased upon consoling and attacking. These results add further evidence that MeA OXT signaling (system) is involved in consolation and aggression.

3) In addition to results described above, apoptosis, pharmacogenetic and pharmacological experiment also support that OXTR and the OXT signaling in these OXTR-expressing neurons are involved in consolation and aggression.

4) Moreover, many previous studies have proven that OXT causally regulate social attachment such as paternal behaviors^{10, 15}, pair bond¹⁶ and consolation¹⁷ especially that are also consistent with our findings.

5) Surprisingly, recent studies report that knocking out of OXTR gene did not affect parental care and pair bonding in prairie voles. Professor Larry Young explained that oxytocin receptor is less an on-off switch and more a way to finetune responses to social cues. But that doesn't mean it isn't important¹⁸. It indicates that manipulation and conclusion of OXTR gene knocking out by Ledford and Berendzen' group still have great controversy¹⁹. According to social salience hypothesis about OXT²⁰, OXT always allows individuals to maintain a sensitivity to social information in the environment and adjust the social decision-making by increasing attention orienting responses to social objects²¹. In conclusion, OXT may adjust AOB-MeA mediated social behaviors elicited by social-odor information in real time²². These social behaviors include social recognition²³, social preference²⁴ and approach²⁵ ect. These reports are consistent with our conclusion.

1. Wu YE, Hong W. Neural basis of prosocial behavior. *Trends Neurosci* **45**, 749-762 (2022).
2. Qian T, *et al.* A genetically encoded sensor measures temporal oxytocin release from different neuronal compartments. *Nat Biotechnol* **41**, 944-957 (2023).
3. Tervo DG, *et al.* A Designer AAV Variant Permits Efficient Retrograde Access to Projection Neurons. *Neuron* **92**, 372-382 (2016).
4. Surdyka MM, Figiel M. Retrograde capabilities of adeno-associated virus vectors in the central nervous system. *Biotechnologia* **102**, 473-478 (2021).
5. Bohlen MO, *et al.* Adeno-Associated Virus Capsid-Promoter Interactions in the Brain Translate from Rat to the Nonhuman Primate. *Human gene therapy* **31**, 1155-1168 (2020).
6. Yang OJ, *et al.* Evaluating the transduction efficiency of systemically delivered AAV vectors in the rat nervous system. *Frontiers in neuroscience* **17**, 1001007 (2023).
7. Song Y, *et al.* Disinhibition of PVN-projecting GABAergic neurons in AV region in BNST participates in visceral hypersensitivity in rats. *Psychoneuroendocrinology* **117**, 104690 (2020).
8. Nanjappa R, Dilbeck MD, Economides JR, Horton JC. Fundus imaging of retinal ganglion cells transduced by retrograde transport of rAAV2-retro. *Experimental eye research* **219**, 109084 (2022).
9. Weiss AR, Liguore WA, Domire JS, Button D, McBride JL. Intra-striatal AAV2-retro administration leads to extensive retrograde transport in the rhesus macaque brain: implications for disease modeling and therapeutic development. *Scientific reports* **10**, 6970 (2020).
10. He Z, *et al.* Paraventricular Nucleus Oxytocin Subsystems Promote Active Paternal Behaviors in Mandarin Voles. *The Journal of neuroscience : the official journal of the Society for Neuroscience* **41**, 6699-6713 (2021).
11. Lv Z, *et al.* Involvement of Serotonergic Projections from the Dorsal Raphe to the Medial Preoptic Area in the Regulation of the Pup-Directed Paternal Response of Male Mandarin Voles. *Int J Mol Sci* **24**, (2023).
12. Li L, *et al.* Dorsal raphe nucleus to anterior cingulate cortex 5-HTergic neural circuit modulates consolation and sociability. *eLife* **10**, (2021).
13. Hou W, *et al.* Oxytocin treatments or activation of the paraventricular nucleus-the shell of nucleus accumbens pathway reduce adverse effects of chronic social defeat stress on emotional and social behaviors in Mandarin voles. *Neuropharmacology* **230**, 109482 (2023).
14. Tsai NY, *et al.* Trans-Seq maps a selective mammalian retinotectal synapse instructed by Nephronectin. *Nat Neurosci* **25**, 659-674 (2022).
15. Yoshihara C, Numan M, Kuroda KO. Oxytocin and Parental Behaviors. *Current topics in behavioral neurosciences* **35**, 119-153 (2018).
16. Walum H, Young LJ. The neural mechanisms and circuitry of the pair bond. *Nature reviews Neuroscience* **19**, 643-654 (2018).
17. Burkett JP, Andari E, Johnson ZV, Curry DC, de Waal FB, Young LJ. Oxytocin-dependent consolation behavior in rodents. *Science* **351**, 375-378 (2016).
18. Ledford H. CRISPR voles can't detect 'love hormone' oxytocin - but still mate for life. *Nature* **614**, 204-205 (2023).
19. Berendzen KM, *et al.* Oxytocin receptor is not required for social attachment in prairie

- voles. *Neuron* **111**, 787-796.e784 (2023).
20. Shamay-Tsoory SG, Abu-Akel A. The Social Salience Hypothesis of Oxytocin. *Biological psychiatry* **79**, 194-202 (2016).
 21. Menon R, Neumann ID. Detection, processing and reinforcement of social cues: regulation by the oxytocin system. *Nature reviews Neuroscience*, (2023).
 22. Gur R, Tendler A, Wagner S. Long-term social recognition memory is mediated by oxytocin-dependent synaptic plasticity in the medial amygdala. *Biological psychiatry* **76**, 377-386 (2014).
 23. Ferguson JN, Aldag JM, Insel TR, Young LJ. Oxytocin in the medial amygdala is essential for social recognition in the mouse. *The Journal of neuroscience : the official journal of the Society for Neuroscience* **21**, 8278-8285 (2001).
 24. Yao S, Bergan J, Lanjuin A, Dulac C. Oxytocin signaling in the medial amygdala is required for sex discrimination of social cues. *eLife* **6**, (2017).
 25. Arakawa H, Arakawa K, Deak T. Oxytocin and vasopressin in the medial amygdala differentially modulate approach and avoidance behavior toward illness-related social odor. *Neuroscience* **171**, 1141-1151 (2010).

REVIEWER COMMENTS

Reviewer #1 (Remarks to the Author):

As previously stated, the study presents a series of stepwise, perhaps even eloquent, experiments showing regional connections, manipulation of neurons, expression and then activation of using optogenetics and pharmaceutical silencing to refine and understand the role of the medial amygdala and specifically neurons that express oxytocin receptors in the anterior insula and ventral lateral ventral medial hypothalamus. The findings indicate that subgroups of oxytocin receptor expressing neurons within the MeA may be involved in the regulation of both aggression and prosocial interactions dependent upon the group and the region they innervate. The authors have strengthened the findings by including additional experiments in the revision and have been responsive to reviewers' comments.

The manuscript reads much better, but there are still a few minor suggested corrections that would no doubt be addressed by the editorial staff. These include:

Line 41 "Given the facts or Given the fact."

Line 131 observed obviously (Fig. 1c). Adverb should not be used to end a sentence.

Line 161 strongly proved the specific involvement – remove proved strongly support – general we do not consider in science that we "prove".

Line 213 we firstly compared – firstly should not be used. First, we is a better presentation.

Line 603 and 609 – There may be other examples, but abbreviations have not been previously defined for MeApv and MeApd. The MeA has been defined, but not all readers may know that posterior ventral and posterior dorsal are represented by pv and pd. Since these are presented from other works and not presented again, probably just best to just spell out pv and dv.

Reviewer #2 (Remarks to the Author):

The authors have done a good job in addressing all the comments. Please note that in Mei et al. study, the AAV1-cre is used to reveal cells that are connected to the MPOA instead of cells that are downstream of the MPOA.

Reviewer #3 (Remarks to the Author):

I appreciate the additional experiments that the authors have performed in the revision. Although they addressed some of my comments, several major issues were not properly addressed. There are also several new issues related to the newly added data that need to be resolved.

1. The authors have not addressed my comments regarding whether Oxtr signaling in the MeA plays a causal role in regulating consolation or aggression. This can be investigated using an oxytocin antagonist.

2. To address the function of glutamatergic MeA neurons, the authors attempted to use the CaMKII promoter to specifically target these neurons. However, while CaMKII marks excitatory neurons in cortical structures, it is known to be expressed in GABAergic neurons in the amygdala and other subcortical brain areas in rodents (e.g., Hogri 2022 J. Neurosci., Keaveney 2020 J. Neurosci.; Klug 2012 PLOS One). It is therefore critical to use a more specific approach to activate glutamatergic neurons, such as vglut2.

3. As reviewer #2 pointed out, the use of the AAV(2/1) viral strategy for anterograde trans-synaptic labeling, which was originally developed in mice, has not been validated in Mandarin voles. Unlike what the authors claimed in their response to reviewer #2's comments, WGA is not a strictly anterograde tracer and can also travel retrogradely. If there are reciprocal projections between the MeA and AI or VMHvl, the cell bodies that were observed in the AI and VMHvl using these two strategies could reflect AI or VMHvl cells that project to the MeA, instead of cells that

receive synaptic inputs from the MeA. The authors should express a fluorescent marker in the AI and VMHvl and examine whether there are reciprocal axonal projections to the MeA. They should also acknowledge the limitations of the tracing methods in the manuscript.

4. For the behavioral experiments in Fig. 1 and 2, the authors used home-cage interaction as a control. An appropriate control should be a separation-only group, as used in previous studies (e.g., Burkett 2016 Science), to exclude the possibility that the observed effects are merely due to the experimental procedures and handling of the animals.

5. Please show the quantification of allogrooming behavior in the consolation assays using male siblings.

6. In Fig. 3b, l, 4c, q, S11b, i, S13b, s, S15b, t, please present images showing the actual fiber tracts instead of schematics, to allow assessment of fiber placement.

7. For histological images (Fig. 2j-l, n-p, 3c, 5d, 6a-d, o), please show individual channels separately (can be shown in the supplement) to allow a better assessment of the overlap between different channels.

8. Fig. 4q, 6n, please show representative images of axonal projections in AI and VMHvl and fiber tracts.

9. In Fig. 2i, OXTR-ir was not defined. In addition, the images in Fig. 2g, h show a nearly complete abolishment of GFP signal, but the quantification of OXTR signal in Fig.2i shows a considerable number of remaining cells. Why is there such a discrepancy?

Point-to-point responses:

(Reviewers' comments in Blue; Our responses in Black)

PS: All changes in the revised manuscript text file are marked with red underline.

Reviewer #1 (Remarks to the Author):

As previously stated, the study presents a series of stepwise, perhaps even eloquent, experiments showing regional connections, manipulation of neurons, expression and then activation of using optogenetics and pharmaceutical silencing to refine and understand the role of the medial amygdala and specifically neurons that express oxytocin receptors in the anterior insula and ventral lateral ventral medial hypothalamus. The findings indicate that subgroups or oxytocin receptor expressing neurons within the MeA may be involved in the regulation of both aggression and prosocial interactions dependent upon the group and the region they innervate. The authors have strengthened the findings by including additional experiments in the revision and have been responsive to reviewers' comments.

Response: Thanks for your positive and valuable comments on our study. With your suggestion and careful checking, the manuscript have been improved significantly. We appreciate your work on our manuscript very much.

The manuscript reads much better, but there are still a few minor suggested corrections that would no doubt be addressed by the editorial staff. These include:

Line 41 "Given the facts or Given the fact."

Response: Thanks for your careful checking. This error has been corrected in the revised manuscript: "Given the facts ..." → "Given the fact ..." (**Pages 2, line 42**).

Line 131 observed obviously (Fig. 1c). Adverb should not be used to end a sentence.

Response: Thanks for your careful checking. This error has been corrected in the revised manuscript: "... mCherry in the MeA were observed obviously" → "... mCherry were obviously observed in the MeA" (**Pages 5, line 137**).

Line 161 strongly proved the specific involvement – remove proved strongly support – general we do not consider in science that we "prove".

Response: Thanks for your suggestion. This error has been corrected in the revised manuscript: "These results strongly proved the ..." → "These results strongly supported the" (**Pages 5, line 169**).

Line 213 we firstly compared – firstly should not be used. First, we is a better presentation.

Response: Thanks for your suggestion. The "firstly" was removed to ensure a better presentation: "... we firstly compared OXTR neurons" → "...we compared OXTR neurons" (**Pages 5, line 221**).

Line 603 and 609 – There may be other examples, but abbreviations have not been previously defined for MeApv and MeApd. The MeA has been defined, but not all readers may know that posterior ventral and posterior dorsal are represented by pv and pd. Since these are presented from other works and not presented again, probably just best to just spell out pv and dv.

Response: Thanks for your suggestion. The “PV (pv)” and “PD (pd)” mentioned in the manuscript have been replaced with the “posterior ventral” and “posterior dorsal”, respectively.

Point-to-point responses:

(Reviewers' comments in Blue; Our responses in Black)

PS: All changes in the revised manuscript text file are marked with red underline.

Reviewer #2 (Remarks to the Author):

The authors have done a good job in addressing all the comments. Please note that in Mei et al. study, the AAV1-cre is used to reveal cells that are connected to the MPOA instead of cells that are downstream of the MPOA.

Response: Thanks again for your professional suggestion and positive comments. With your help, the present study has been significantly improved. I have carefully read the manuscript of Mei et al. study and corrected my misunderstanding. In the future, I will pay more attention to the application of anterograde cross-synaptic virus tracing strategies.

To eliminate the possible false positive results caused by the limitations of the virus strategy (AAV1 and mWGA) itself, we injected the rAAV2/9-CAG-EGFP-WPRE-hGh-pA in the AI and VMHvl and observed rare axon projections to the MeA from the AI and VMHvl (**Fig. S8 in manuscript**). This result confirmed the high effectiveness and credibility of the anterograde monosynaptic AAV (2/1) and AAV (mWGA) tracing strategies used for this study.

Point-to-point responses:

(Reviewers' comments in Blue; Our responses in Black)

PS: All changes in the revised manuscript text file are marked with red underline.

Reviewer #3 (Remarks to the Author):

I appreciate the additional experiments that the authors have performed in the revision. Although they addressed some of my comments, several major issues were not properly addressed. There are also several new issues related to the newly added data that need to be resolved.

Response: Thanks for your professional suggestions. These suggestions are helpful and valuable for improving our works. We made response to your comments one by one as following.

1. The authors have not addressed my comments regarding whether Oxt signaling in the MeA plays a causal role in regulating consolation or aggression. This can be investigated using an oxytocin antagonist.

Response: Thanks for your valuable suggestion. The additional pharmacological experiment had been conducted in the revised version.

For exploring whether OXTR signaling in the MeA plays a causal role in regulating consolation or aggression, we blocked OXTR function in the MeA by infusion of vehicle containing an OXTR antagonist (OXTR-A, ([d (CH₂) 51, Tyr (Me) 2, Thr₄, Orn₈, des-Gly-NH₂]-Vasotocin trifluoroacetate salt, 0.5 ng / 200 nl per side ^{1, 2, 3}) to the bilateral MeA. The consoling performance in consolation test and aggressive behavior in resident-intruder paradigm were recorded.

As showed in the following **Fig. S15 in manuscript**, OXTR-A administration to the MeA decreased both levels of consolation and aggression. Corresponding results have been added in **pages 9, line 244-249**. Corresponding method for this experiment has been added in **pages 34, line 898-909**. Combined with increased OXT release and increased activities of the MeA^{OXTR+AI} among subjects when encountering distressed siblings and of the MeA^{OXTR+VMHvl} among subjects when encountering intruders (**Fig. S16 in the manuscript**), and obvious effects of optogenetic and chemogenetic manipulation of the MeA^{OXTR+AI} on levels of consolation and MeA^{OXTR+VMHvl} on levels of aggression (**Fig. 3 ~ 6 in the manuscript**), we can confirm with certainty that both the OXTR signaling in the MeA and the two populations of MeA^{OXTR} cells are necessary in regulating consolation and aggression.

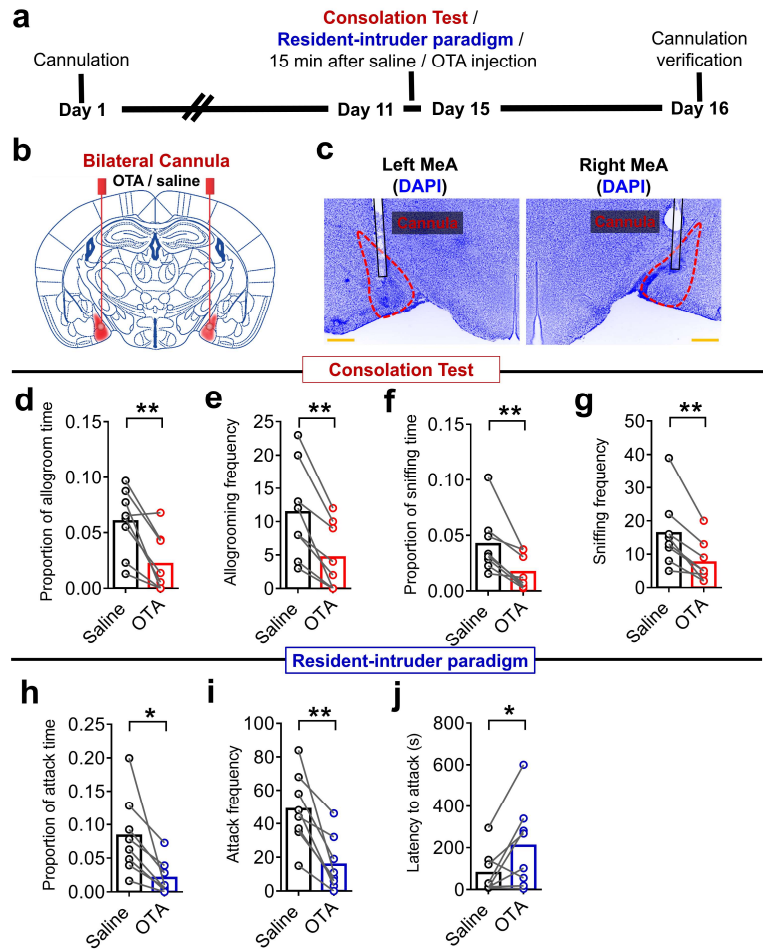


Fig. S15 | The effect of microinjection of OXTR antagonists in the bilateral MeA on consolation and aggression behaviors. a–c Diagram showing experimental schedule (a), schematic representation of MeA infusion sites (b) and representative photomicrograph of the injection site (c). scale bars, 500 μ m. d–g Quantitative distinction of duration proportion and frequency of allogrooming and sniffing between the saline and OTA groups. h–j Quantitative distinction of duration proportion and frequency of attack, and latency to attack between the saline and OTA groups. ** $p < 0.01$, * $p < 0.05$. All error bars = s.e.m.

2. To address the function of glutamatergic MeA neurons, the authors attempted to use the CaMKII promoter to specifically target these neurons. However, while CaMKII marks excitatory neurons in cortical structures, it is known to be expressed in GABAergic neurons in the amygdala and other subcortical brain areas in rodents (e.g., Hogri 2022 J. Neurosci., Keaveney 2020 J. Neurosci.; Klug 2012 PLOS One). It is therefore critical to use a more specific approach to activate glutamatergic neurons, such as vglut2.

Response: Thanks for your suggestion. To address this issue, the additional experiment was conducted. As showed in **Fig. 6l ~ z and Fig. S26 in the manuscript**, we directly activated fibers located in the AI or VMHvl of the glutamatergic (VGlut2)-MeA^{OXTR} neurons, and corresponding results have been added in **pages 21, line 498-pages 22, line 516**. These results indicated that optogenetic activation of glutamatergic (VGlut2)-MeA^{OXTR+AI} and MeA^{OXTR+VMHvl} fibers were sufficient to increase levels of consolation and aggression, respectively.

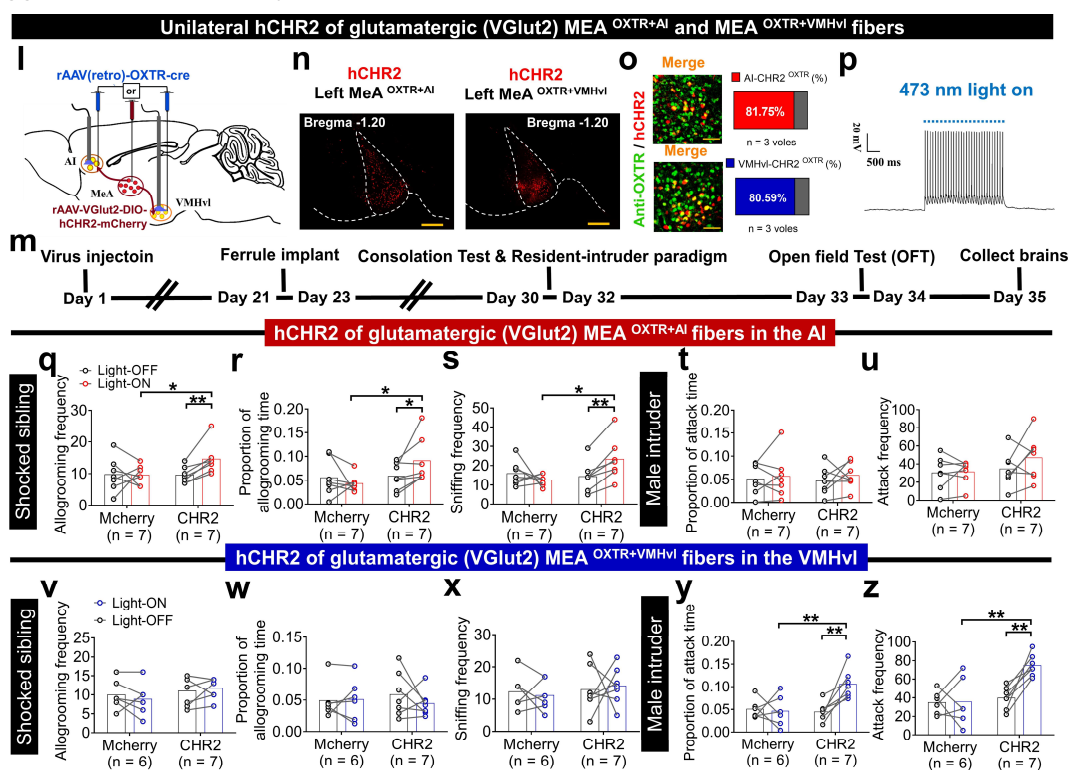


Fig. 6l ~ z in manuscript | Optogenetic activation of the glutamatergic (VGlut2)-MeA^{OXTR+AI} and MeA^{OXTR+VMHvl} fibers facilitated consolation and aggression **l, m** Virus regimen (**l**) and schedule (**m**) for optogenetic activation of the glutamatergic (VGlut2) fibers of the MeA^{OXTR+AI} and MeA^{OXTR+VMHvl}. **n** Images of hChR2 expression (red). scale bars, 500 μm. **o** Representative overlapped images of VGlut2-hChR2 somata and anti-OXTR cells. scale bars, 50 μm; Statistical charts showed AI- and VMHvl-projecting hChR2 neurons were relatively restricted to anti-OXTR cells. n = 3 voles / group. **p** Representative electrophysiological traces showing photoactivation effect. **q-u, and v-z** Comparison of allogrooming (**q, r, v** and **w**) and sniffing siblings (**s** and **x**), and attacking intruders (**t, u, y** and **z**) between the VGlut2-hChR2 and VGlut2-mCherry groups in the MeA^{OXTR+AI} and MeA^{OXTR+VMHvl}. n = 6-7 voles in each group in (**q-z**). ***p < 0.001, **p < 0.01, *p < 0.05. All error bars = s.e.m.

3. As reviewer #2 pointed out, the use of the AAV(2/1) viral strategy for anterograde trans-synaptic labeling, which was originally developed in mice, has not been validated in Mandarin voles. Unlike what the authors claimed in their response to reviewer #2's comments, WGA is not a strictly anterograde tracer and can also travel retrogradely. If there are reciprocal projections between the MeA and AI or VMHvl, the cell bodies that were observed in the AI and VMHvl using these two strategies could reflect AI or VMHvl cells that project to the MeA, instead of cells that receive synaptic inputs from the MeA. The authors should express a fluorescent maker in the AI and VMHvl and examine whether there are reciprocal axonal projections to the MeA. They should also acknowledge the limitations of the tracing methods in the manuscript.

Response: Thanks for your suggestion.

In the method section, we added a statement that the limitations of these two virus strategies that AAV1 (cre-DIO system) and mWGA (CAG promotor) viral strategy are not strictly anterograde tracers and may produce less retrograde traces. Corresponding methods were added in **pages 32, line 801-line 802**.

To eliminate the possible false positive results caused by the limitations of the virus strategy itself, we used a new virus strategy in the revised version for further explanation. We expressed rAAV2/9-CAG-EGFP-WPRE-hGh-pA in the AI / VMHvl for 30 days in male mandarin voles as showed in **Fig. S8 in manuscript** according to your suggestion, and we found that there was rare axon projection to the MeA from the AI and VMHvl (**Fig. S8b and d in manuscript**). This result can indicate that the AAV2/1 (cre-DIO system) and mWGA (CAG promoter) strategies and their corresponding results are largely credible. Corresponding results have been added in **pages 5 line 166-168**. Corresponding methods text was showed in **pages 32 line 802-807**.

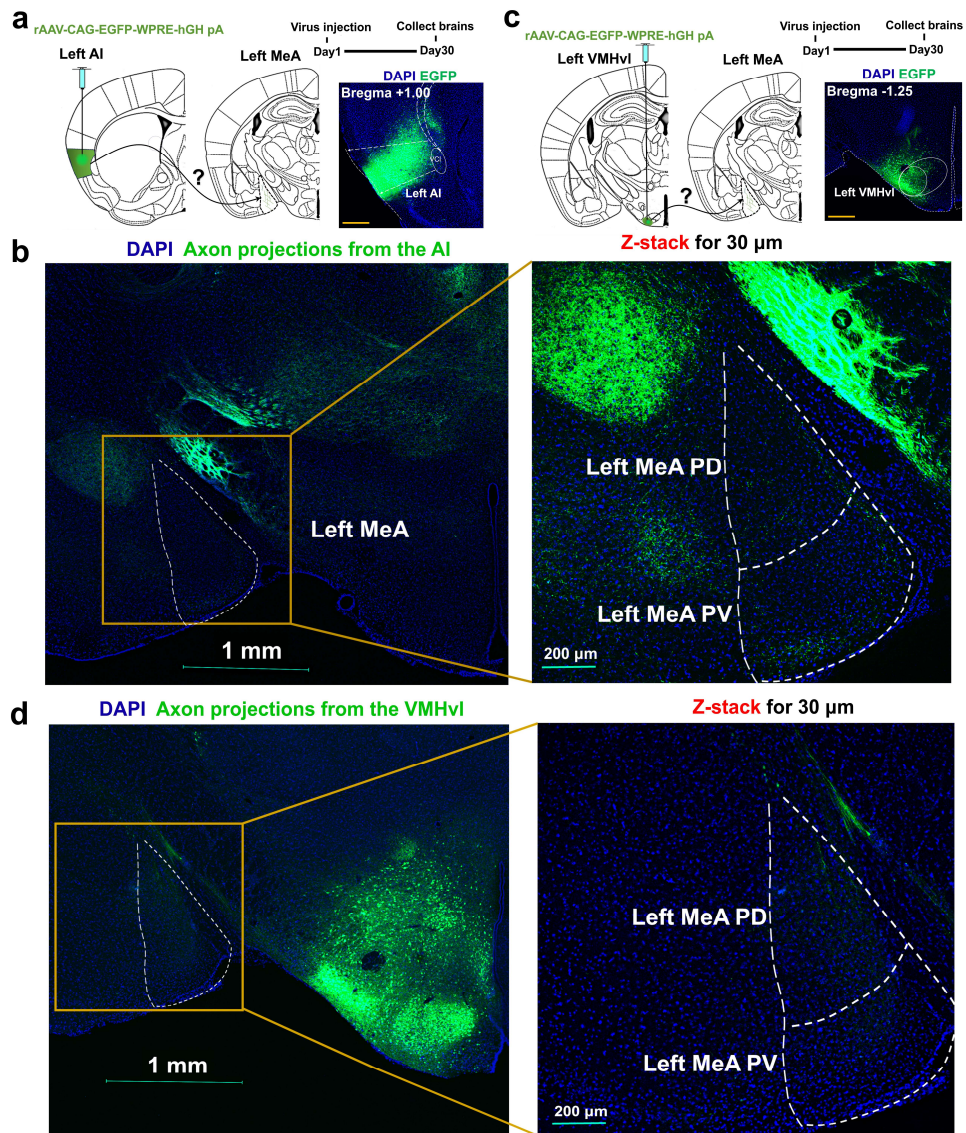
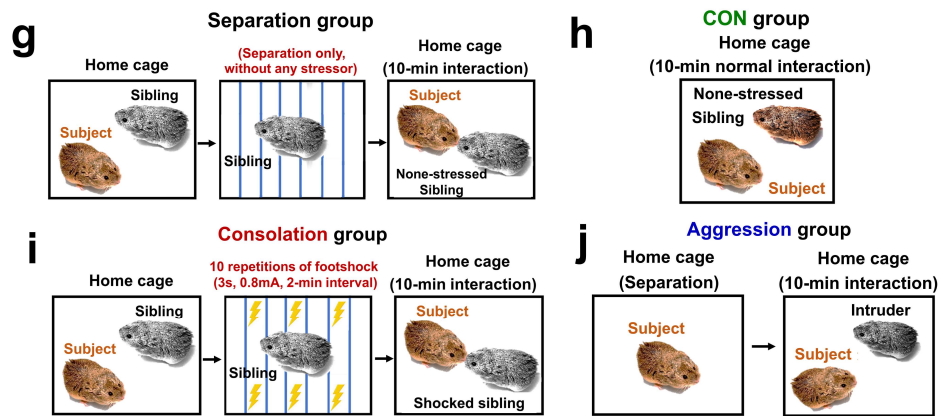


Fig. S8 | Confirmation the rare existence of axonal projections to the MeA from the AI and VMHvl using AAV2/9-type anterograde virus carrying EGFP florescence, respectively. a, c Diagram showing virus injection regimen (left), schedule (up right) and representative images of rAAV injection site (up down). scale bars, 500 µm. **b, d** Representative 30µm Z-stack images of axonal fibers (EGFP, green) to the MeA from the AI and VMHvl. scale bars, 1000 µm (left) and 200 µm (right).

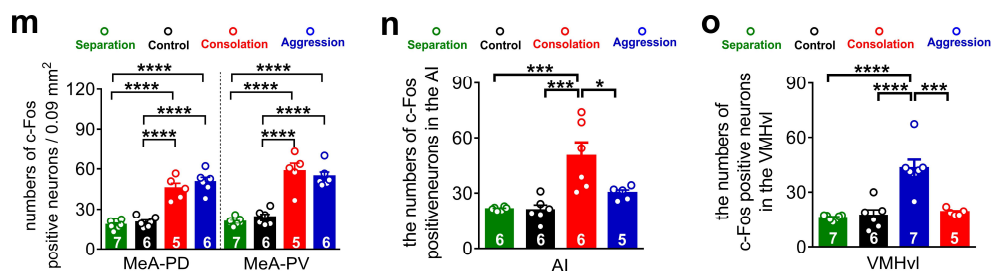
4. For the behavioral experiments in Fig. 1 and 2, the authors used home-cage interaction as a control. An appropriate control should be a separation-only group, as used in previous studies (e.g., Burkett 2016 Science), to exclude the possibility that the observed effects are merely due to the experimental procedures and handling of the animals.

Response: Thanks for your suggestion.

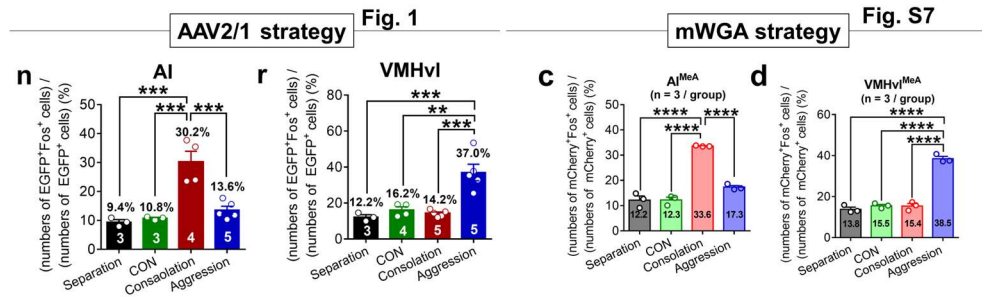
To address this issue, we added Separation group ^{1,4} in (1) “Quantification of c-Fos expression of the MeA, AI and VMHvl under consolation and aggression”, (2) “Quantification of c-Fos expression of the AI^{MeA} and VMHvl^{MeA} neurons marked by anterograde monosynaptic virus strategy (AAV1 and mWGA) under consolation and aggression” and (3) “Quantification of c-Fos expression of the MeA^{OxTR+AI} and MeA^{OxTR+VMHvl} neurons under consolation and aggression” experiments. The processing flow for the four groups (CON, Separation, Consolation and Aggression groups) is as showed in **Fig. 1g ~ j in manuscript**:



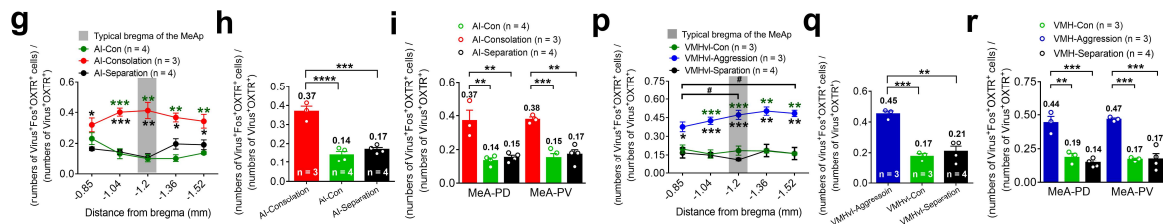
In experiment (1), the Separation group and CON group (home-cage interaction group) didn't show any difference in levels of c-Fos expression in the MeA PD, MeA PV, AI and VMHvl than (**Fig. S3m ~ o in manuscript**). Corresponding results have been added in **pages 4 line 114-125**. Corresponding methods text was showed in **pages 30 line 735-749**.



In experiment (2), the Separation group and CON group didn't show any difference in levels of c-Fos expression in the AI^{MeA} and VMHvl^{MeA} than the CON group (Fig. 1, and Fig. S5 and S6 for AAV1 strategy; Fig. S7 for mWGA strategy in manuscript). Corresponding results have been added in pages 5 line 149-158. Corresponding methods text was showed in pages 31 line 770-779.



In experiment (3), the Separation group and the [home-cage interaction](#) group didn't show any difference in levels of c-Fos expression in the MeA^{AI+OXTR} and MeA^{VMHvl+OXTR} (Fig. S21 in manuscript). If we used separation group as control, the analysis result is same as that using [home-cage interaction](#) as a control. Corresponding results have been added in pages 13 line 336-344. Corresponding methods text was showed in pages 33 line 850-861.



5. Please show the quantification of allogrooming behavior in the consolation assays using male siblings.

Response: Thanks for your professional suggestion. For addressing this question, there are several points that needed to be explained here.

(1) Based on previous observations of the behaviors of distressed demonstrators (partners or siblings) in consolation tests conducted in our lab^{5,6,7}, it can be concluded that demonstrator voles showed very rare or even no consoling behaviors towards the subjects. This result is consistent with Weizhe Hong's research findings⁴.

(2) For verifying this conclusion in this study

① On the one hand, we referred Weizhe Hong's refined analysis and analyzed demonstrators' behavior in this study⁴. Thus, we compared prosocial (allogrooming, sniffing and social approach) and non-social behaviors (self-grooming and rearing) from stressed male siblings (demonstrators) upon encountering subjects (observers) in different groups (EGFP group vs. Casp3 group as an example). As showed in **Fig. S14a ~ j in manuscript**, we found that there was no any difference in allogrooming, sniffing, social approach and self-grooming behaviors between AI(VMHvl)-EGFP and AI(VMHvl)-Casp3 groups.

<1> Similar levels of allogrooming (sniffing) in siblings (demonstrators) between groups could exclude effects of different consoling level of siblings on levels of allogrooming of subjects.

<2> Similar levels of social approach of siblings (demonstrators) between groups could exclude the effects of different levels of help-seeking behaviors of siblings on levels of allogrooming in subjects.

<3> Similar levels of self-grooming behavior of siblings (demonstrators) between groups could exclude effects of self-grooming in siblings on allogrooming of subjects.

In addition, sibling demonstrators in AI-Casp3 group showed more rearing than AI-EGFP groups (**Fig. S14e and j in manuscript**). Such increased anxious behavior in siblings in AI-Casp3 group may be caused by less consolation given by subjects after apoptosis of the MeA^{OXTR+AI}.

② On the other hand, the subjects showed definitely more allogrooming behaviors than their corresponding siblings in the AI-EGFP (but not AI-Casp3), VMHvl-EGFP and VMHvl-Casp3 groups (**Fig. S14k ~ n in manuscript**). This result directly indicated that the allogrooming behavior of sibling demonstrators may not affect the subjects' consolation behaviors. It should be noticed that no difference of allogrooming frequency in the AI-Casp3 group between subjects and siblings may be due to apoptosis of the MeA^{OXTR+AI} in subjects that may significantly reduce levels of consolation behaviors (**Fig. S14l in manuscript**).

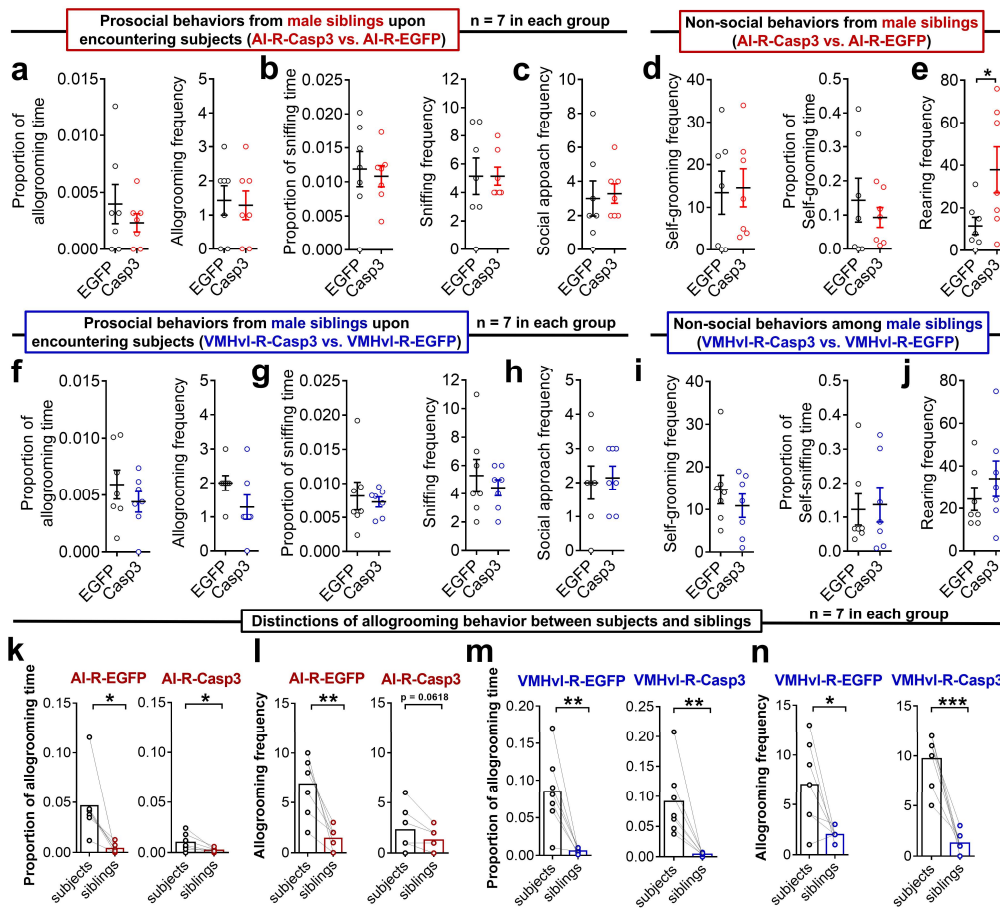
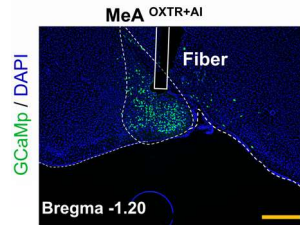


Fig. S14 | Prosocial and non-social behavioral performance from the male stressed siblings upon encountering subjects in consolation assays in the apoptosis experiment. a–c, and f–h Quantitative distinction of duration proportion and frequency of allogrooming and sniffing, and frequency of social approach from male siblings between the AI-retro EGFP and Casp3 groups (a–c) or between the VMHv1-retro EGFP and Casp3 groups (f–h). **d, e, i and j** Quantitative distinction of duration proportion and frequency of self-grooming, and frequency of rearing from male siblings between the AI-retro EGFP and Casp3 groups, or between the VMHv1-retro EGFP and Casp3 groups (i and j). **k–n** Quantitative distinction of duration proportion and frequency of allogrooming between male siblings and subjects in the AI-retro EGFP, AI-retro Casp3, VMHv1-retro EGFP and VMHv1-retro Casp3 groups. *** $p < 0.001$, ** $p < 0.01$, * $p < 0.05$. All error bars = s.e.m.

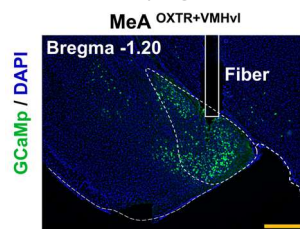
6. In Fig. 3b, l, 4c, q, S11b, i, S13b, s, S15b, t, please present images showing the actual fiber tracts instead of schematics, to allow assessment of fiber placement.

Response: According to your professional suggestion, all merged images of actual fiber tracts and successful viral expression have been added in corresponding figures and supplementary figures (scale bars, 500 μm).

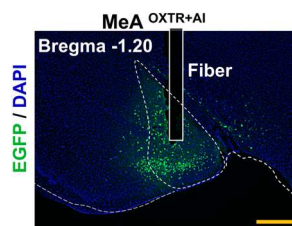
(1). GcaMP6m of the MeA^{OXTR+AI} cells (**Fig. 3b in manuscript**)



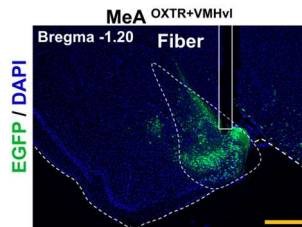
(2). GcaMP6m of the MeA^{OXTR+VMHvl} cells (**Fig. 3l in manuscript**)



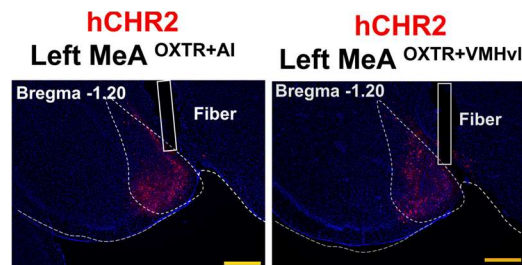
(3). EFPG (control for GcaMP6m) of the MeA^{OXTR+AI} cells (**Fig. S20b in manuscript**)



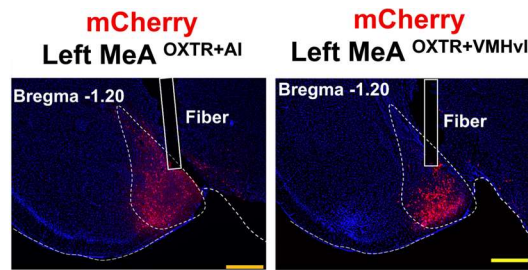
(4). EFPG (control for GcaMP6m) of the MeA^{OXTR+VMHvl} cells (**Fig. S20t in manuscript**)



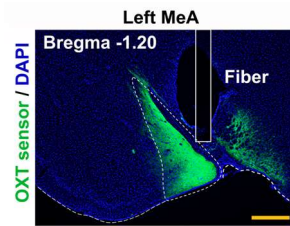
(5). hCHR2 of the MeA^{OXTR+AI} and MeA^{OXTR+VMHvl} somata (**Fig. 4c in manuscript**)



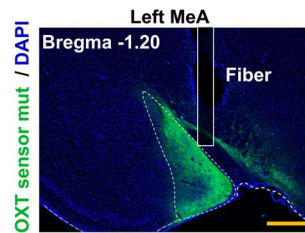
(6). mCherry (control for hCHR2) of the MeA^{OxTR+AI} and MeA^{OxTR+VMHvl} somata (Fig. S22b in manuscript)



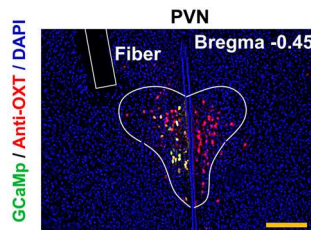
(7). OXT sensor in the MeA (Fig. S16b in manuscript)



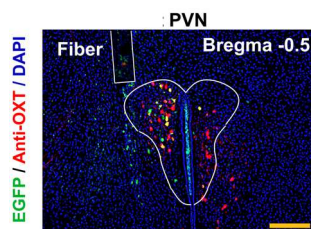
(8). OXT sensor mut in the MeA (Fig. S18b in manuscript)



(9). GcaMP6m of the PVN^{OxT+MeA} cells (Fig. S16l in manuscript)



(10). EGFP (control for GcaMP6m) of the PVN^{OxT+MeA} cells (Fig. S18s in manuscript)



7. For histological images (Fig. 2j-l, n-p, 3c, 5d, 6a-d, o), please show individual channels separately (can be shown in the supplement) to allow a better assessment of the overlap between different channels.

Response: According to your professional suggestion, all images of individual channels have been added in supplementary figures.

(1). Activated AI^{MeA} cells under four treatments marked by AAV1 virus strategy and c-Fos.

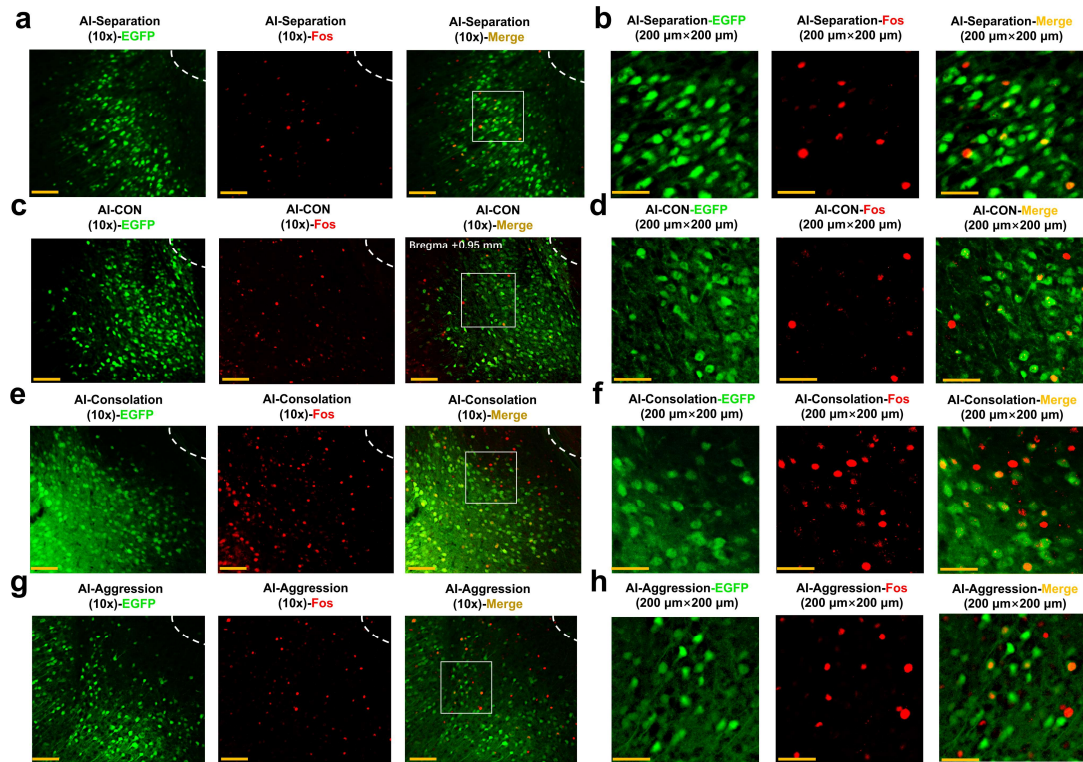


Fig. S5 | The corresponding individual channels' images (left) from representative overlapped images (right) of anterograde virus and c-Fos at the AI (AI^{MeA+Fos}) in the Separation, CON, Consolation and Aggression groups. The enlarged views of the selected white boxed areas (200 μm×200 μm, right). scale bars, 100 μm (left) and 50 μm (right).

(2). Activated VMHv^{MeA} cells under four treatments marked by AAV1 virus strategy and c-Fos.

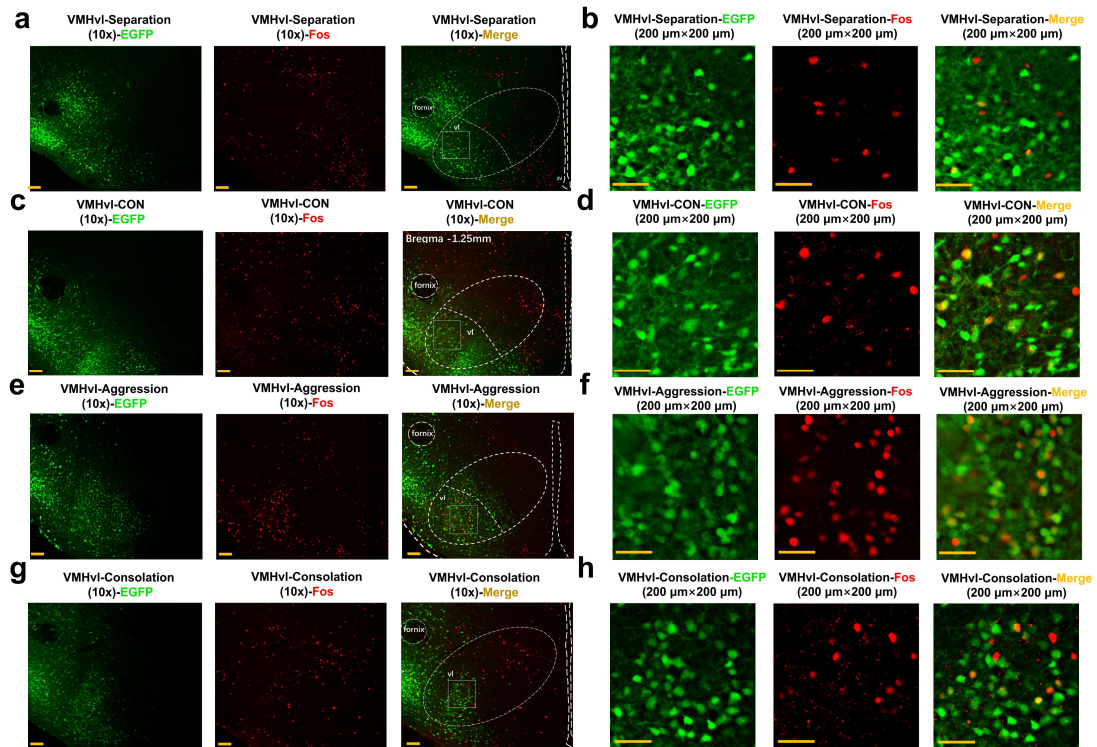


Fig. S6 | The corresponding individual channels' images (left) from representative overlapped images (right) of anterograde virus and c-Fos at the VMHv (VMHv^{MeA+Fos}) in the Separation, CON, Consolation and Aggression groups. The enlarged views of the selected white boxed areas (200 μm×200 μm, right). scale bars, 100 μm (left) and 50 μm (right).

(3). MeA^{OXTR+AI+VMHvl} cells

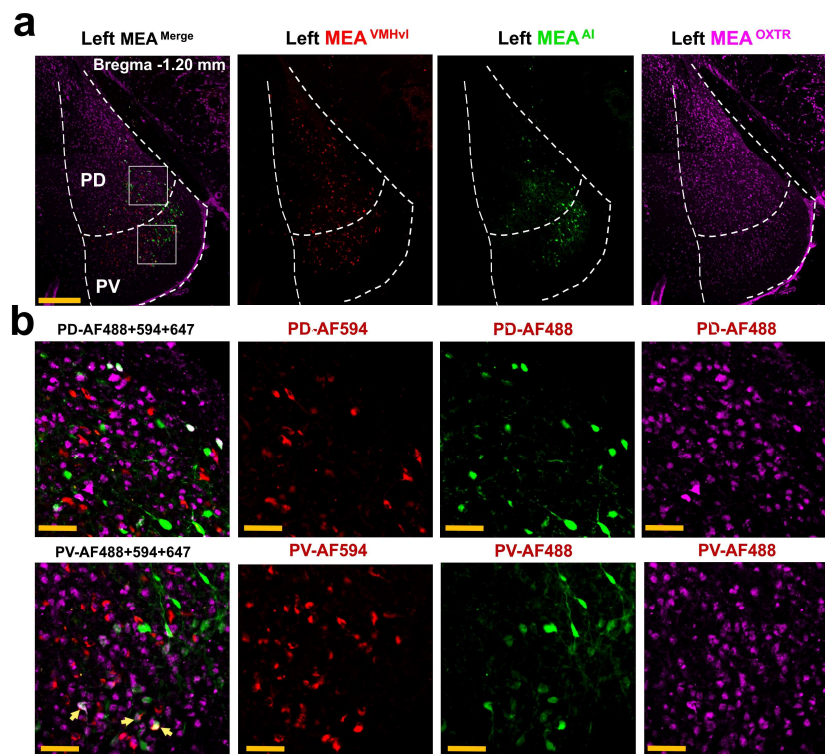


Fig. S10 | The corresponding individual channels' images (right) from representative overlapped images of MeA^{OXTR+AI+VMHvl} (left) and the proportion of MeA^{AI}, MeA^{VMHvl}, MeA^{AI+VMHvl} expressing OXTR along the anteroposterior axis at the PD and PV subregions. The enlarged views of the selected white boxed areas (200 μ m \times 200 μ m, right) in b. scale bars, 200 μ m in a and 50 μ m in b. ** $p < 0.01$, * $p < 0.05$. All error bars = s.e.m.

(4) hCHR2 of MeA^{OXTR+AI(VMHvl)} somata and mCherry (control of hCHR2) of MeA^{OXTR+AI(VMHvl)} somata

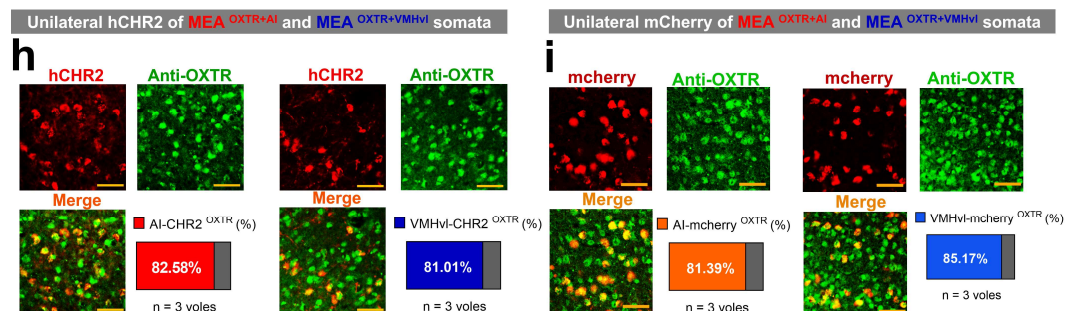


Fig. S22 | Effects of optogenetic activation of somata of the MeA^{OXTR+AI} and MeA^{OXTR+VMHvl} on anxiety level and locomotion. **h, i** The corresponding individual channels' images from representative overlapped images of hCHR2-MeA^{OXTR+AI} and hCHR2-MeA^{OXTR+VMHvl} somata, and overlapped images of mCherry-MeA^{OXTR+AI} and mCherry-MeA^{OXTR+VMHvl} somata. scale bars, 50 μ m.

(5) hCHR2 of MeA^{OXTR+AI(VMHvl)} fibers and mCherry (control of hCHR2) of MeA^{OXTR+AI(VMHvl)} fibers

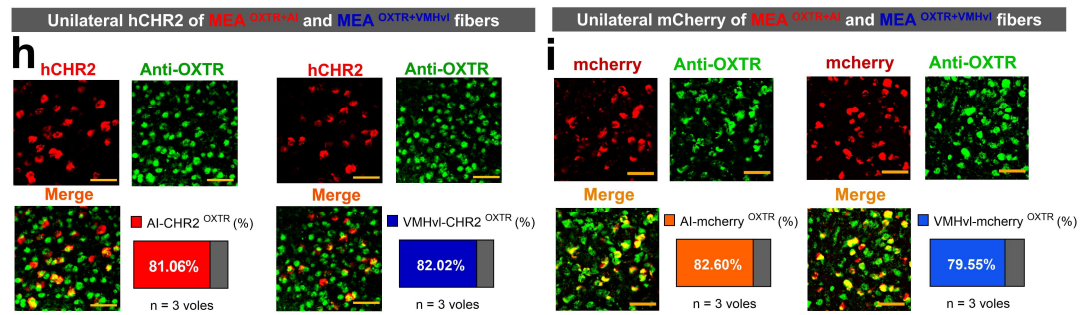


Fig. S23 | Effects of optogenetic activation of fibers of the MeA^{OXTR+AI} and MeA^{OXTR+VMHvl} on anxiety level and locomotion. **h, i** The corresponding individual channels' images from representative overlapped images of hCHR2-MeA^{OXTR+AI} somata and anti-OXTR cells and overlapped images of hCHR2-MeA^{OXTR+VMHvl} somata and anti-OXTR cells, and overlapped images of mCherry-MeA^{OXTR+AI} somata and anti-OXTR cells and overlapped images of mCherry-MeA^{OXTR+VMHvl} somata and anti-OXTR cells. scale bars, 50 μm.

(6) Gi of MeA^{OXTR+AI(VMHvl)} cells and mCherry (control of Gi) of MeA^{OXTR+AI(VMHvl)} cells

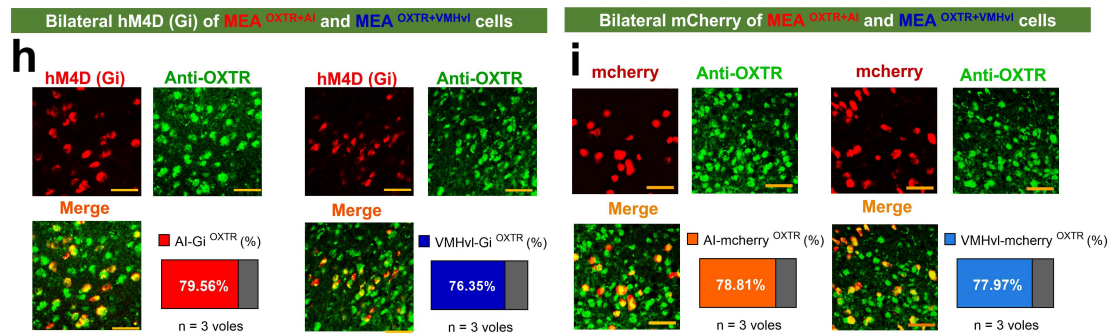


Fig. S24 | Effects of pharmacogenetic inhibition of the MeA^{OXTR+AI} and MeA^{OXTR+VMHvl} on anxiety level and locomotion. **h, i** The corresponding individual channels' images from representative overlapped images of hM4D(Gi)-MeA^{OXTR+AI} and hM4D(Gi)-MeA^{OXTR+VMHvl} somata, and mCherry-MeA^{OXTR+AI} and mCherry-MeA^{OXTR+VMHvl} somata. scale bars, 50 μm.

(7) Main type of the MeA^{OXTR+AI(VMHvl)} neurons

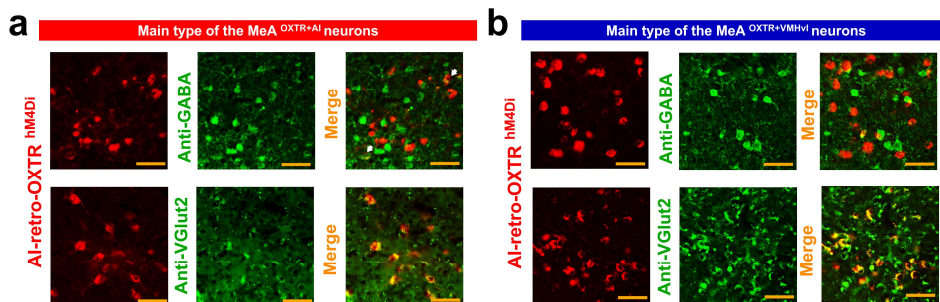


Fig. S25 | The corresponding individual channels' images from representative overlapped images of hM4Di (Gi) and VGlut2 positive neurons, and Gi and GABA positive neurons in the MeA^{OXTR+AI} and MeA^{OXTR+VMHvl}. scale bars, 50 μm.

(8) VGlut2-hCHR2 of MeA^{OXTR+AI(VMHvl)} fibers and VGlut2-mCherry (control of VGlut2-hCHR2) of MeA^{OXTR+AI(VMHvl)} fibers

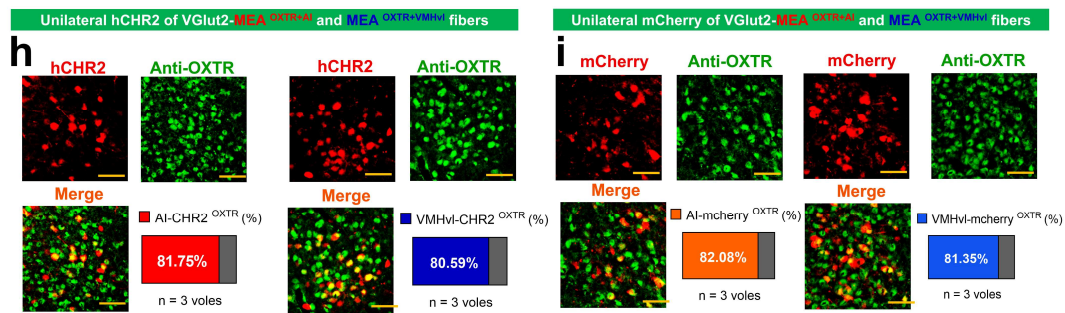


Fig. S26 | Effects of optogenetic activation of fibers of the glutamatergic (VGlut2) MeA^{OXTR+AI} and MeA^{OXTR+VMHvl} on anxiety level and locomotion. h, i The corresponding individual channels' images from representative overlapped images of hCHR2 (VGlut2)-MeA^{OXTR+AI} somata and anti-OXTR cells and overlapped images of hCHR2 (VGlut2)-MeA^{OXTR+VMHvl} somata and anti-OXTR cells, and overlapped images of mCherry (VGlut2)-MeA^{OXTR+AI} somata and anti-OXTR cells and overlapped images of mCherry (VGlut2)-MeA^{OXTR+VMHvl} somata and anti-OXTR cells. scale bars, 50 μm.

(9) CAMKIIα-hCHR2 of MeA^{OXTR+AI(VMHvl)} fibers and CAMKIIα-mCherry (control of CAMKIIα-hCHR2) of MeA^{OXTR+AI(VMHvl)} fibers

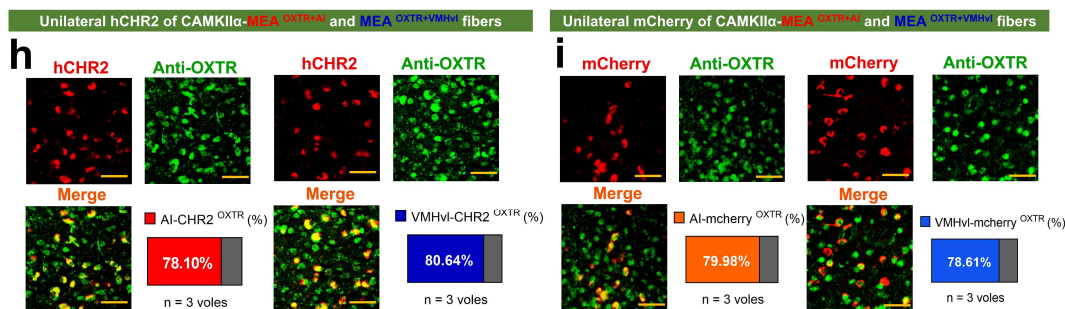


Fig. S28 | Effects of optogenetic activation of fibers of the glutamatergic (CAMKIIα) MeA^{OXTR+AI} and MeA^{OXTR+VMHvl} on anxiety level and locomotion. h, i The corresponding individual channels' images from representative overlapped images of hCHR2 (CAMKIIα)-MeA^{OXTR+AI} somata and anti-OXTR cells and overlapped images of hCHR2 (CAMKIIα)-MeA^{OXTR+VMHvl} somata and anti-OXTR cells, and overlapped images of mCherry (CAMKIIα)-MeA^{OXTR+AI} somata and anti-OXTR cells and overlapped images of mCherry (CAMKIIα)-MeA^{OXTR+VMHvl} somata and anti-OXTR cells. scale bars, 50 μm.

8. Fig. 4q, 6n, please show representative images of axonal projections in AI and VMHvl and fiber tracts.

Response: According to your professional suggestion, all representative merged images of axon projections and fiber tracts have been added in supplementary figures.

(1). hCHR2 of MeA^{OXTR+AI(VMHvl)} fibers and mCherry (control of hCHR2) of MeA^{OXTR+AI(VMHvl)} fibers

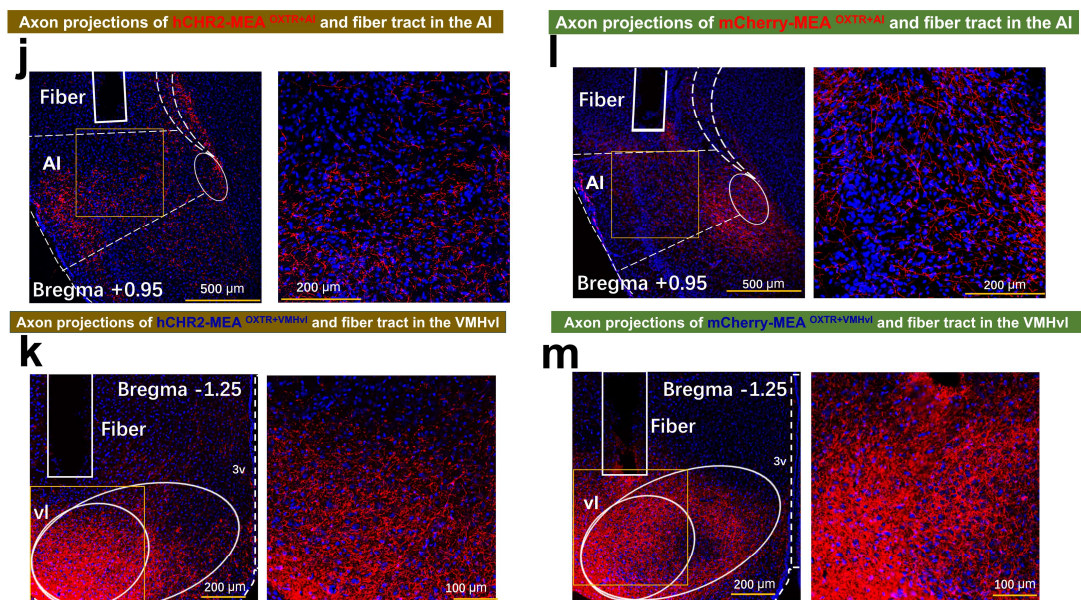


Fig. S23 | Effects of optogenetic activation of fibers of the MeA^{OXTR+AI} and MeA^{OXTR+VMHvl} on anxiety level and locomotion. j, k Representative axon projections and fiber tract of hCHR2-MeA^{OXTR+AI} and hCHR2-MeA^{OXTR+VMHvl} in the AI and VMHvl. **l, m** Representative axon projections and fiber tract of mCherry-MeA^{OXTR+AI} and MeA^{OXTR+VMHvl} in the AI and VMHvl. scale bars, 500 μm (left) and 200 μm (right) in j and l; 200 μm (left) and 100 μm (right) in k and m.

(2). VGlut2-hCHR2 of MeA^{OXTR+AI(VMHvl)} fibers and VGlut2-mCherry (control of VGlut2-hCHR2) of MeA^{OXTR+AI(VMHvl)} fibers

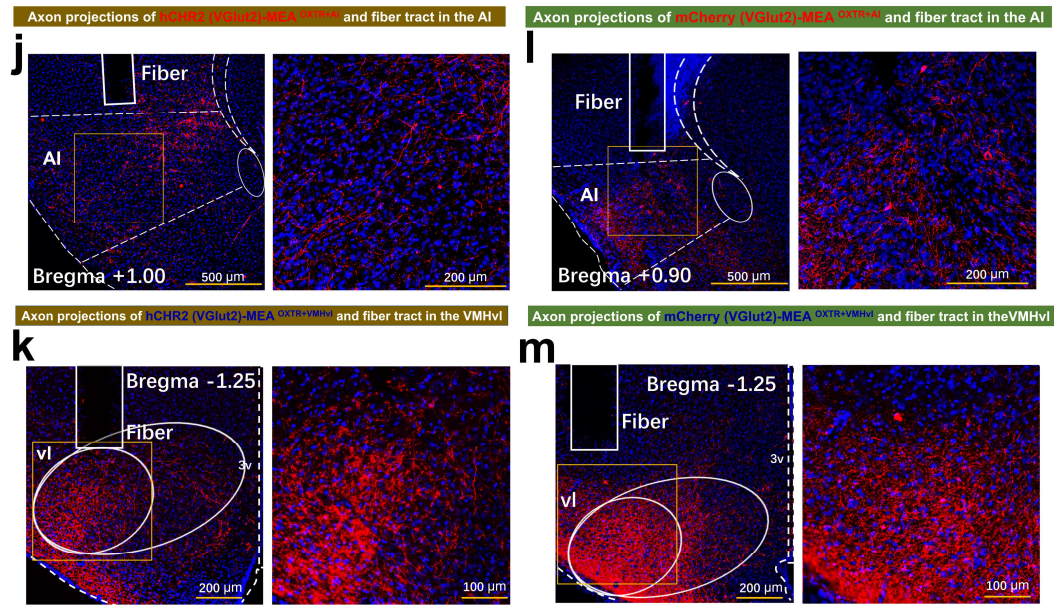


Fig. S26 | Effects of optogenetic activation of fibers of the glutamatergic (VGlut2) MeA^{OXTR+AI} and MeA^{OXTR+VMHvl} on anxiety level and locomotion. j, k Representative axon projections and fiber tract of VGlut2-hCHR2-MeA^{OXTR+AI} and VGlut2-hCHR2-MeA^{OXTR+VMHvl} in the AI and VMHvl. **l, m** Representative axon projections and fiber tract of VGlut2-mCherry-MeA^{OXTR+AI} and VGlut2-mCherry-MeA^{OXTR+VMHvl} in the AI and VMHvl. scale bars, 500 μm (left) and 200 (right) in j and l; 200μm (left) and 100 (right) in k and m.

(3). CAMKII α -hCHR2 of MeA^{OXTR+AI}(VMHvl) fibers and CAMKII α -mCherry (control of CAMKII α -hCHR2) of MeA^{OXTR+AI}(VMHvl) fibers

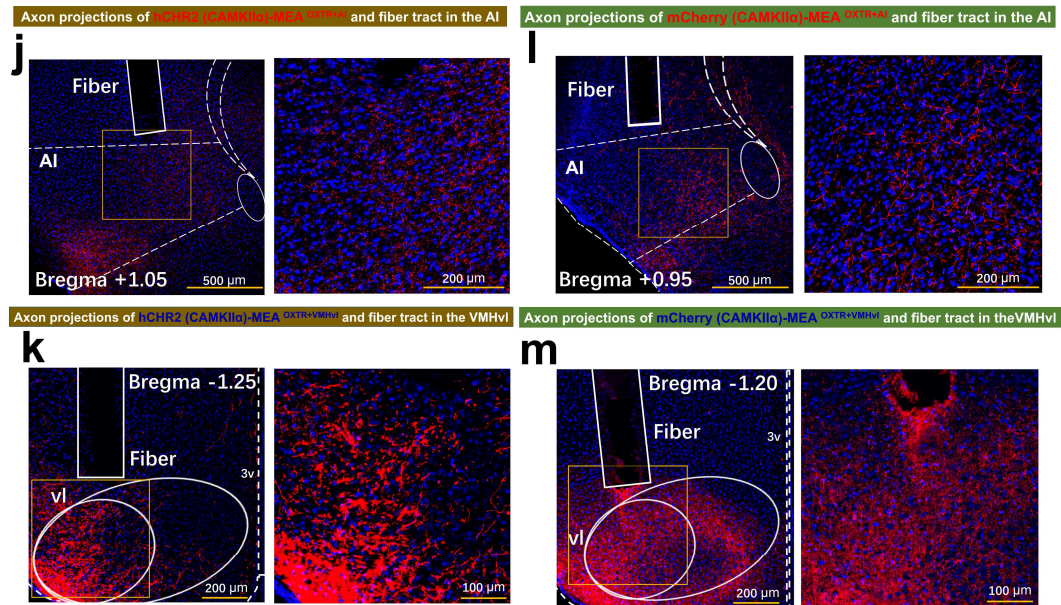


Fig. S28 | Effects of optogenetic activation of fibers of the glutamatergic (CAMKII α) MeA^{OXTR+AI} and MeA^{OXTR+VMHvl} on anxiety level and locomotion. j, k Representative axon projections and fiber tract of CAMKII α -hCHR2-MeA^{OXTR+AI} and CAMKII α -hCHR2-MeA^{OXTR+VMHvl} in the AI and VMHvl. **l, m** Representative axon projections and fiber tract of CAMKII α -mCherry-MeA^{OXTR+AI} and CAMKII α -mCherry-MeA^{OXTR+VMHvl} in the AI and VMHvl. scale bars, 500 μ m (left) and 200 (right) in j and l; 200 μ m (left) and 100 (right) in k and m.

9. In Fig. 2i, OXTR-ir was not defined. In addition, the images in Fig. 2g, h show a nearly complete abolishment of GFP signal, but the quantification of OXTR signal in Fig. 2i shows a considerable number of remaining cells. Why is there such a discrepancy?

Response: Sorry for the confusion that the information between **Fig. 2g, h** and **Fig. 2i** in the previous version of the manuscript is different. **Fig. 2g, h (previous version)** showed the virus expression from Caps3-EGFP and EGFP (control for Casp3) groups while Caps3-EGFP display less EGFP while EGFP (control for Casp3) showed very dense EGFP. However, **Fig. 2i (previous version)** showed numbers of OTR positive neurons.

To eliminate the confusion, we have replaced the figure that only display virus expression of Caps3 with figure that display OTR and virus co-labeled images in the latest version of the manuscript. Here is an explanation and improvement.

For verifying cre-dependent death of the $\text{MeA}^{\text{OXTR+AI}}$ or $\text{MeA}^{\text{OXTR+VMHvl}}$ in the apoptosis experiment,

(1). we observed the Caps3-EGFP and EGFP (control for Casp3) viral expression, the representative images were showed in **Fig. S12** in the current version of the manuscript.

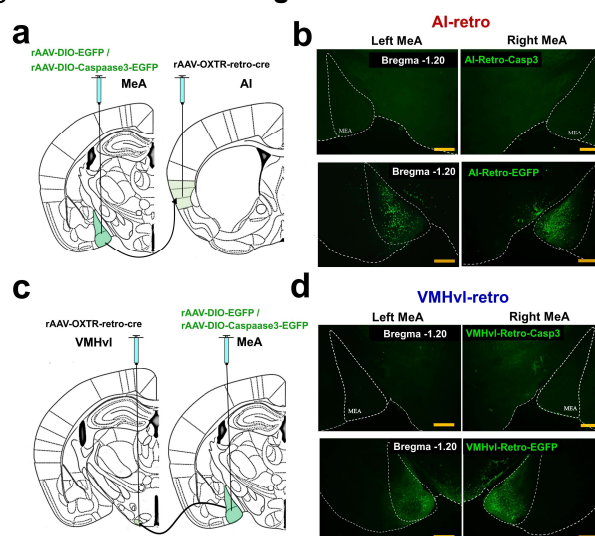


Fig. S12 | Diagram showing protocol of virus injection for apoptosis experiment (a and c) and representative images of bilateral Casp3-EGFP (up) and EGFP (down) expression in the $\text{MeA}^{\text{OXTR+AI}}$ and $\text{MeA}^{\text{OXTR+VMHvl}}$. scale bars, 500 μm.

(2). We then evaluate the effect of apoptosis of specific pathway (AI / VMHvl projecting MeA^{OXTR} neurons) on the numbers of OXTR-ir neurons (definition: the MeA neurons stained by OXTR antibody) between the EGFP and Casp3 groups. The representative individual channel images of both EGFP and corresponding OXTR-ir cells were showed in **Fig. 2g and h** in the current version of the manuscript.

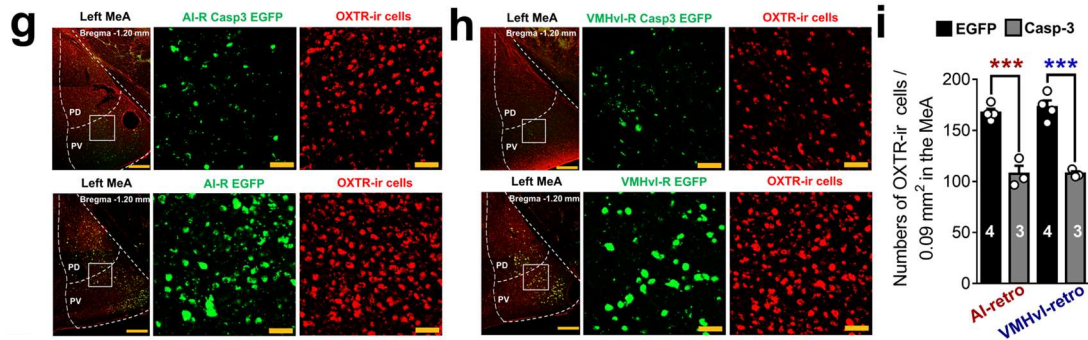


Fig. 2 | Distribution of the MeA^{OXTR+AI} and MeA^{OXTR+VMHvl} and effects of apoptosis of these two populations of neurons on consolation and aggression. g, h Representative co-labeling images of AI-retro / VMHvl-retro Caspase3 or EGFP (green) and anti-OXTR (OXTR-ir cells, red) in the MeA (left). The enlarged views of the selected white boxed areas (300 μm \times 300 μm , right). scale bars, 200 μm (left) and 50 μm (right). i Numbers distinction / 0.09 mm² of OXTR-ir cells in the MeA between the AI-retro EGFP and Casp3 groups, and between the VMHvl-retro EGFP and Caspase3 groups. ***p < 0.001. All error bars = s.e.m.

Therefore, **Fig. 2i in the manuscript** show numbers of the rest MeA^{OXTR} neurons after apoptosis of MeA^{OXTR+AI} or MeA^{OXTR+VMHvl} neurons rather than numbers of the MeA cells marked by (Casp3)-EGFP. In the current version of the manuscript, the images of the OXTR-ir cells in the four groups (Fig. 2 g h) were presented to match the results of the difference analysis in **Fig. 2i**. The figures may be easier to be understood now.

Reference

- Burkett JP, Andari E, Johnson ZV, Curry DC, de Waal FB, Young LJ. Oxytocin-dependent consolation behavior in rodents. *Science* **351**, 375-378 (2016).
- Ferguson JN, Aldag JM, Insel TR, Young LJ. Oxytocin in the medial amygdala is essential for social recognition in the mouse. *The Journal of neuroscience : the official journal of the Society for Neuroscience* **21**, 8278-8285 (2001).
- Samuelsen CL, Meredith M. Oxytocin antagonist disrupts male mouse medial amygdala response to chemical-communication signals. *Neuroscience* **180**, 96-104 (2011).
- Wu YE, *et al.* Neural control of affiliative touch in prosocial interaction. *Nature* **599**, 262-267 (2021).
- Li L, *et al.* Dorsal raphe nucleus to anterior cingulate cortex 5-HTergic neural circuit modulates consolation and sociability. *eLife* **10**, (2021).
- Li LF, *et al.* Reduced Consolation Behaviors in Physically Stressed Mandarin Voles: Involvement of Oxytocin, Dopamine D2, and Serotonin 1A Receptors Within the Anterior Cingulate Cortex. *Int J Neuropsychopharmacol* **23**, 511-523 (2020).
- Li LF, *et al.* Involvement of oxytocin and GABA in consolation behavior elicited by socially defeated individuals in mandarin voles. *Psychoneuroendocrinology* **103**, 14-24 (2019).

REVIEWER COMMENTS

Reviewer #3 (Remarks to the Author):

The authors have done an excellent job in addressing all my comments. In particular, I am very pleased that the authors are able to activate VGlut2+ neurons using VGlut2-DIO-hChR2 viruses. To my knowledge, VGlut2-DIO-hChR2 AAV was almost never used and is not validated in the manuscript. It is therefore essential to validate the expression of VGlut2-DIO-hChR2 to make sure that it is indeed expressed specifically in glutamatergic neurons. The authors can do this by co-injecting/expressing it with AAV-syn-Cre, and co-stain infected cells with VGlut2 and VGat antibodies (and quantify the overlap). This is a minor experiment, but it is essential to support the main conclusion of the paper, given how rarely this virus was used before. Another minor comment is that the authors should provide representative videos to show optogenetically induced consolation and aggression (for optogenetics experiments in both Figures 4 and 6) in the supplemental materials.

Point-to-point responses:

(Reviewers' comments in Blue; Our responses in Black)

PS: All changes in the revised manuscript text file are marked with red underline.

Reviewer #3 (Remarks to the Author):

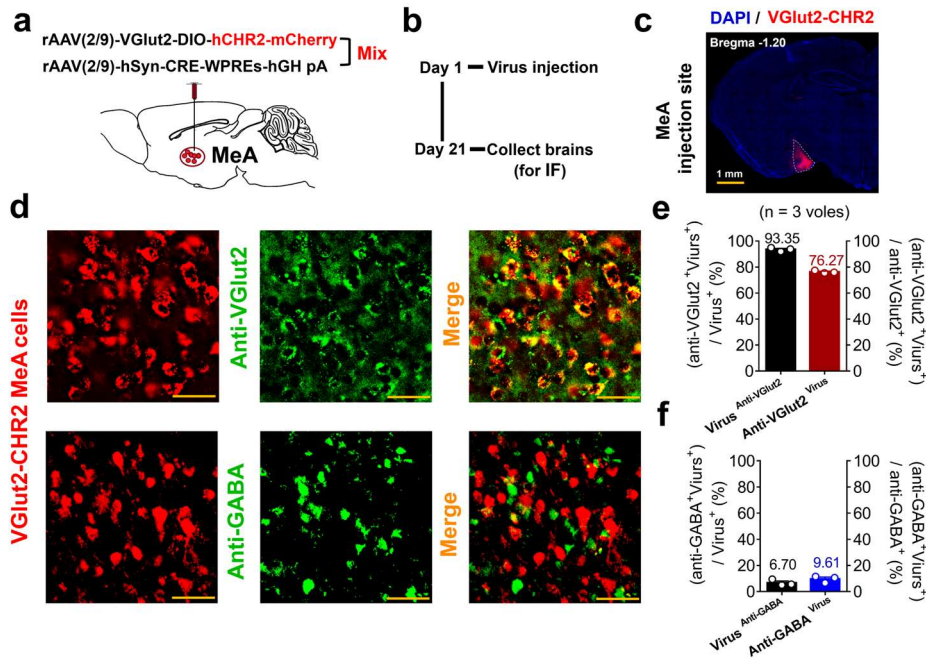
The authors have done an excellent job in addressing all my comments. In particular, I am very pleased that the authors are able to activate VGlut2+ neurons using VGlut2-DIO-hChR2 viruses.

Response: Thank you very much for your positive comment on our work. Your professional suggestions are helpful and valuable for improving our study. We made response to your comments one by one as following.

To my knowledge, VGlut2-DIO-hChR2 AAV was almost never used and is not validated in the manuscript. It is therefore essential to validate the expression of VGlut2-DIO-hChR2 to make sure that it is indeed expressed specifically in glutamatergic neurons. The authors can do this by co-injecting/expressing it with AAV-syn-Cre, and co-stain infected cells with VGlut2 and VGat antibodies (and quantify the overlap). This is a minor experiment, but it is essential to support the main conclusion of the paper, given how rarely this virus was used before.

Response: I agree with your suggestion that VGlut2-DIO-hChR2 AAV should be validated. According your suggestion, we injected mixture of rAAV-VGlut2-DIO-hCHR2 (2/9) and rAAV-CRE (2/9) to the MeA as shown in **Supplementary Fig. 26** in supplementary information file. These two viruses were designed and constructed to specifically infect the glutamatergic neurons. 21 days later after virus injection, the brains were collected and cut with freezing microtome, and brain slices were stained with VGlut2 and GABA antibodies (**Supplementary Fig. 26a-c**). The result shows that approximately 93.35% of virus infected cells were labeled by VGlut2 antibody and only 6.70% of infected cells were labeled by GABA antibody. In addition, these viruses could infect 76.27% of the whole glutamatergic MeA neurons (**Supplementary Fig. 26e and f**).

We therefore demonstrated the high specificity and efficiency of the virus infection. This result indicates that the viruses used to activate glutamatergic neurons are valid and would also support our main conclusion. Corresponding results have been added in **pages 21, line 422-426**. Corresponding method for this experiment has been added in **pages 32, line 766-773**.



Supplementary Fig. 26 | The validation of the efficiency and specificity of rAAV-VGlut2-DIO-hChr2-mCherry infection in the MeA. (a) and (b) Virus regimen (a) and schedule (b) were used to infect the glutamatergic (VGlut2⁺) MeA neurons by co-injecting rAAV-VGlut2-DIO-hChr2 with rAAV-hSyn-Cre into the MeA. **(c)** Representative image of VGlut2-mCherry expression (red) in the left MeA. scale bars, 1 mm. **(d)** Representative images of VGlut2-CHR2⁺ infected neurons and Anti-VGlut2⁺ / Anti-GABA⁺ labeled cells in the MeA. scale bars, 50 μ m. **(e) and (f)** Quantification of the percentage of VGlut2 (GABA) antibody-labeled VGlut2-CHR2⁺ neurons in the total VGlut2-CHR2⁺ infected cells, and quantification of the percentage of VGlut2-CHR2⁺ infected cells in the total VGlut2 / GABA antibody-labeled cells. All error bars = s.e.m

Another minor comment is that the authors should provide representative videos to show optogenetically induced consolation and aggression (for optogenetics experiments in both Figures 4 and 6) in the supplemental materials.

Response: Thanks for your suggestions. We have added representative videos of three optogenetic experiments in the supplemental materials. From these videos, the readers can intuitively find that optogenetic activation of somata or (glutamatergic) fibers of the MeA^{OXTR+AI} and MeA^{OXTR+VMHvl} can effectively induce the occurrence of consolation and aggressive behaviors, respectively.